Available online at www.sciencedirect.com
ScienceDirect
Marine and Petroleum Geology 24 (2007) 289–311
Marine and Petroleum Geology
www.elsevier.com/locate/marpetgeo

Experimental mechanical compaction of clay mineral aggregates—Changes in physical properties of mudstones during burial

Nazmul H. Mondol*, Knut Bjørlykke, Jens Jahren, Kaare Høeg

Department of Geosciences, University of Oslo, P.O. Box 1047, Blindern N-0316, Oslo, Norway

Received 6 November 2006; received in revised form 5 March 2007; accepted 7 March 2007

Abstract

Dry and brine-saturated clay aggregates ranging from pure smectite to pure kaolinite were compacted in the laboratory. Experiments were conducted by increasing vertical effective stress up to 50 MPa to study the changes in physical properties of mudstones during burial. The results suggest that the physical properties (porosity, density, acoustic velocity, etc.) of mudstones vary greatly with increasing effective stress, clay mineralogy and fluid content. Kaolinite aggregates are much more compressible than those composed of smectite. Brine-saturated clay mixtures are much more compressible than dry clay mixtures. Brine may soften and lubricate the clay matrix compared to dry clays, resulting in higher compressibility in the brine-saturated state. The lesser degree of compaction of dry smectite compared to dry kaolinite aggregates can be explained by the differences in grain size as kaolinitic clays have much larger grains than smectitic clays. The extremely fine-grained nature of smectite implies that the imposed vertical stress is distributed over a very large number of grain contacts so that the force per contact area is very low in smectite compared to that in coarse-grained kaolinite. At 20 MPa effective stress, corresponding to about 2 km burial depth with hydrostatic pore pressure, brine-saturated pure kaolinite compacted to 20% porosity, while pure smectite retained 41% porosity. Brine-saturated clay mixtures show higher V_p and lower V_s than dry clay mixtures. A pronounced difference in V_s was observed among the brine-saturated clay mixtures. The lowest V_s as a function of vertical effective stress was found for pure smectite. For a given porosity value, smectitic clays have higher velocities and elastic moduli than the kaolinitic clays. The V_p/V_s ratio is significantly higher in smectite than in kaolinite aggregates. Treating mudstones as a uniform class of rocks introduces significant errors in estimates of physical properties, which are strongly affected by the clay mineralogy, grain size, the amount of other minerals present and fluid content. Our results have implications for well log interpretation and mudstone and shale property determinations from seismic data at shallow burial depth (<2 km, 80 °C), above depths where significant chemical compaction takes place.

Keywords: Mechanical compaction; Effective stress; Clay minerals; Smectite; Kaolinite; Mudstones; Acoustic velocity; Velocity ratio

1. Introduction

Sediment compaction is an important phenomenon in sedimentary basins causing changes in physical properties of the sediments during burial. The resulting changes in physical properties such as porosity, density and velocity with depth are complex functions of mechanical and chemical compaction processes. Mechanical compaction of fine-grained clayey sediments is different from that of sands and carbonates (Athy, 1930; Weller, 1959; Magara, 1980; Sclater and Christie, 1980; Baldwin and Butler, 1985; Chuhan et al., 2003). Clays and muds have higher porosity at the time of deposition and are therefore affected more by the mechanical compaction than other sediments. This leads to pronounced changes in physical properties of mudstones with increasing stress or depth of burial. Mechanical compaction is a function of effective stress and dominates in the shallow parts of the basin down to 2–4 km depth (80–100 °C) depending on the geothermal gradient. Chemical compaction, including dissolution and precipitation of minerals, dominates in the deeper parts of

*Corresponding author. Tel.: +47 2285 4224; fax: +47 2285 4215.
E-mail addresses: nazmul.haque@geo.uio.no (N.H. Mondol), knut.bjorlykke@geo.uio.no (K. Bjørlykke), jens.jahren@geo.uio.no (J. Jahren), kaare.hoeg@geo.uio.no (K. Høeg).

0264-8172/$ - see front matter © 2007 Elsevier Ltd. All rights reserved.
doi:10.1016/j.marpetgeo.2007.03.006

the basin at higher temperatures (>80–100 °C), where time, temperature and mineralogy are the principle controls on compaction (Bjørlykke, 1997; Bjørkum et al., 1998; Bjørlykke, 1999; Lander and Walderhaug, 1999; Storvoll et al., 2005). Chemical compaction of mudstones is difficult to investigate in the laboratory due to slow kinetics, but mechanical compaction can readily be simulated to gain better understanding of the compaction behavior of mudstones. The primary components of mudstones are various types of clay minerals of which smectite and kaolinite are important constituents. They represent end members compared to other clay minerals (illite, chlorite, etc.) in terms of grain size, surface area and cation exchange capacity. Smectite is the most fine-grained clay found in nature, has high cation exchange capability and large surface area; while kaolinite is course-grained and has lower cation exchange capacity and smaller surface area (Meade, 1963; Mesri and Olson, 1971; Rieke and Chilingarian, 1974).

Understanding of the physical and elastic properties of clays and mudstones with progressive burial is also important for petroleum exploration, drilling and production. The presence of a small amount of clays in carbonates and sandstones has large influence on their physical properties and reduce the mobility of reservoir fluids. Clay-rich sediments are the important source rocks for hydrocarbon generation and behave as efficient seals for trapping hydrocarbon. There is an increasing awareness that changes in physical properties of mudstones associated with petroleum production have strong impact on seismic velocities. Thus, the present laboratory investigation of mechanical compaction of clays also have significant importance for seismic imaging, since stress-related changes in acoustic properties of thick mudstones and shale layers affect seismic wave propagation.

A number of studies describing mudstone and shale compaction have been published over the past 80 years (Rubey, 1927; Jones, 1944; Skempton, 1944; Ham, 1966; Magara, 1968; Skempton, 1970; Baldwin, 1971; Durmishyan, 1974; Magara, 1980; Larsen and Chilingar, 1983; Dzevanshir et al., 1986; Bayer and Wetzel, 1989; Issler, 1992; Karig and Hou, 1992; Aplin et al., 1995; Vasseur et al., 1995; Hansen, 1996; Velde, 1996; Pouya et al., 1998; Yang and Aplin, 1998; Nygard et al., 2004; Aplin and Larter, 2005; Aplin et al., 2006). A variety of empirical relationships has been proposed to express the compaction behavior of mudstones and shales as a function of increasing stress or depth of burial (Terzaghi, 1925; Athy, 1930; Hedberg, 1936; Dickinson, 1953; Rubey and Hubbert, 1959; Weller, 1959; Chilingar and Knight, 1960; Hamilton, 1976b; Baldwin and Butler, 1985; Burland, 1990; Goulty, 1998; Yang and Aplin, 2004). Fig. 1 shows a group of published porosity-depth trends of mudstones and shales from different part of the world suggested. The general aspects of the compaction of mudstones and shales have been adequately discussed by previous authors and they need not be repeated here.

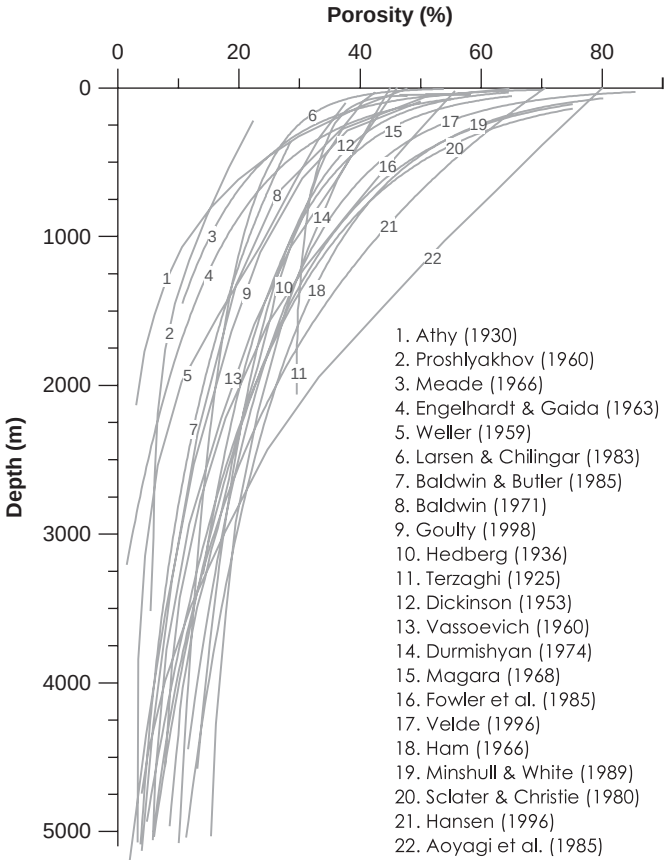

Fig. 1. Compaction curves for shales and argillaceous sediments. The curves are selected from available published porosity–depth trends from different parts of the world.

So far, only a few studies have been reported on compaction of pure clays (Bolt, 1956; Chilingar and Knight, 1960; Mitchell, 1960; Olson and Mitronovas, 1962; Engelhardt and Gaida, 1963; Meade, 1966; Chilingarian and Rieke, 1968; Wijeyesekera and DeFreitas, 1976; Aoyagi et al., 1985; Djeran et al., 1998). Bolt (1956) has shown the physico-chemical effects and compressibility of clays. Chilingar and Knight (1960) studied the relationship between the moisture content and the applied pressure for kaolinite, illite and montmorillonite clays. Mitchell (1960) verified the applicability of colloidal theory to the compressibility of clays. Olson and Mitronovas (1962) measured the shear strength and consolidation characteristics for calcium and magnesium illite. Engelhardt and Gaida (1963) compressed pure montmorillonite and kaolinite with solutions of NaCl and $CaCl_2$ and suggested that the influence of electrolyte concentration on equilibrium porosity is significant under low to moderate overburden stress only. Meade (1966) investigated the petrologic and geochemical factors influencing compaction of clayey sediments. Chilingarian and Rieke (1968) showed relationship of pressure and moisture content of different clay minerals (halloysite, hectorite, dickite, etc.) in addition to results of Chilingar and Knight (1960). Remoulded and undisturbed samples of kaolinite were compacted by

Wijeyesekera and DeFreitas (1976) for understanding fabric and chemistry of the expelled pore fluid. Aoyagi et al. (1985) investigated the compaction behavior of Na-montmorillonite mixed with seawater and crude oil to understand primary oil migration from source rocks. Djeran et al. (1998) compacted remoulded and natural clays under stress ranging from 0.1 to 50 MPa to understand the compaction behavior of different clay minerals.

In addition to compaction, the better understanding of the acoustic properties of clays, mudstones and shales with progressive burial is very important for petroleum exploration, drilling and production. In the past, various model have been proposed for relationships between porosity, acoustic velocity and stress or depth of burial of clastic sediments (Wood, 1941; Faust, 1951; Wyllie et al., 1956; Laughton, 1957; Nafe and Drake, 1957; Shumway, 1958; Geertsma, 1961; Geertsma and Smit, 1961; Pickett, 1963; Hottmann and Johnson, 1965; Gardner et al., 1974; Raymer et al., 1980; Tosaya, 1982; Domenico, 1984; Castagna et al., 1985; Han et al., 1986). Velocities and elastic parameters for mudstones, shaley sandstones, sandy shales and shales as a function of effective stress were also investigated by Tosaya and Nur (1982), Kowallis et al. (1984), Han (1986), Klimentos (1991), Marion et al. (1992), Berge and Berryman (1995), Hornby (1998) and Hornby et al. (2000). A series of investigations of the relationship among velocity, porosity and depth in marine sediments was performed (Hamilton, 1971; Hamilton, 1976a; Nobes et al., 1986; Ayres and Theilen, 1999; Dvorkin et al., 1999; Prasad and Dvorkin, 2001). Predicting S-wave velocity is very important for seismic modeling, amplitude-versus-offset analyses and other exploration applications. Measured S-wave logs are, however, often unavailable. Thus, various theoretical and empirical formulations for S-wave estimation in porous rocks are suggested in the literature (Kuster and Toksoz, 1974a; O'Connell and Budiansky, 1974; Castagna et al., 1985; Han et al., 1986; Krief et al., 1990; Greenberg and Castagna, 1992; Xu and White, 1996; Wang, 2000). These have had limited success, because velocity depends on many factors such as rock composition, effective stress, pore shape distribution, pore fluid, pore pressure etc (Mindlin, 1949; Gassmann, 1951; Biot, 1956; Hashin and Shtrikman, 1963).

Data on velocity and elastic parameters for clay minerals are relatively scarce. Kaarsberg (1959), Alexandrov and Ryzhova (1961), Katahara (1996), Mese and Tutuncu (1996), Wang et al. (2001), and Vanorio et al. (2003) measured velocities and elastic moduli of clay minerals but little agreement is shown among the measurements. Mudstones and shales make up nearly 75% of most sedimentary basins and overlie most petroleum reservoirs (Sayers, 1994; Hornby, 1998; Domnesteanu et al., 2002). Successful imaging of the reservoir intervals depends on correct parameters describing the wave propagation through the overlying shaley sequences. The existing shale velocity database suggests that seismic propagation through shales is a function of the intrinsic anisotropy of the clay minerals (Banik, 1984; Hornby et al., 1994; Vernik and Liu, 1997), compliance between clay minerals (Sayers, 1994) and their microstructure (Rai and Hanson, 1988; Vernik and Nur, 1992). Velocities in clay-matrix supported silisiclastic sediments are also sensitive to the chemistry of the fluids saturating their pore spaces (King, 1966; Liu et al., 1994) and the stress state (Jones and Wang, 1981; Johnston, 1987) over the whole porosity range found in mudstones and shales.

1.1. Scope of experimental study

The present experimental study attempts to determine the mechanical compaction and accompanying changes in the acoustic properties of aggregates of pure smectite, kaolinite and their mixtures as a function of vertical effective stress. Both dry and brine-saturated synthetic samples tested up to 50 MPa correspond to about 4.5–5 km burial depth at hydrostatic fluid pressure conditions. Compaction tests could also have been carried out on natural clays and mudstones. However, in a sedimentary basin like the North Sea, cores of shallow mudstones are rare and most sediments buried to 1.5–2 km or more have been subjected to some chemical compaction (cementation) like carbonate cementation. Studies of mechanical compaction alone would be difficult using such samples. It would also have been difficult to analyze the mineralogical and textural composition and to reconstruct the primary constituents in such natural samples. By using artificial clay mineral mixtures, the initial composition prior to compaction is well known and one has the advantage of avoiding any kind of cementation effect. The outcome of the present study will help to model the shallower part of the basins, by extending the existing knowledge of mechanical compaction of mudstones and shales. It may also assist in predicting more reliable porosity/density/velocity versus depth trends for mudstones and shales, data that are extensively used as input parameters for basin modeling. The results can be compared with natural compaction trends observed in sedimentary basins based on well logs, and the degree of cementation and overpressure in the pore fluid can be estimated. Although the compaction behavior of natural clays can differ substantially from the behavior of reconstituted clays, due to the depositional conditions and post-depositional events, still the experimental work has significant importance for understanding the natural process.

2. Materials and methods

The experimental compaction and velocity measurements on dry and brine-saturated clay mixtures were performed at the Norwegian Geotechnical Institute (NGI). The experiments were conducted with a high-stress oedometer (uniaxial strain, i.e. no lateral strain allowed) equipped with acoustic measurements transducers. It is assumed that the individual grain compressibility is negligible compared to

the bulk compressibility of the clays, so that the pore volume changes can be considered equal to the bulk volume changes of the clay samples. Changes in porosity as a function of effective stress were measured from the expelled volume of air or brine for dry and brine-saturated samples, respectively. All experiments were performed at room temperature which was between 19 and 21 °C.

2.1. Samples and sample preparation

A set of 12 synthetic samples (6 dry and 6 brine-saturated) were prepared in the laboratory by mixing known amounts of smectite and kaolinite. The powdered form of smectite and kaolinite were purchased from Potterycraft Ltd., UK. The particle size of kaolinite was within the range of 1–10 μm, whereas the size of smectite particles was less than 0.1 μm. The mineralogical and chemical composition of the smectite and kaolinite were determined by X-ray diffraction (XRD) and X-ray fluorescence (XRF) spectroscopy. The mineralogical and chemical data are presented in Tables 1 and 2. The liquid limit (the fluid content at which a material begins to behave as a liquid) and grain densities were measured in the laboratory by a liquid limit device and a pycnometer, respectively. Oven dried (60 °C for 2–3 days) clay powder was used for the dry tests. For the wet tests, samples were prepared as slurries by mixing clay powder with salt water. Uniformity was obtained by dry mixing before addition of water. The water was collected from the Oslo Fjord and the salinity was about 34,000 ppm (parts per million). Samples were prepared by thoroughly mixing the clays with water, to a water content equal to 1.5 times the liquid limit (Burland, 1990; Callisto and Calabresi, 1998). The clay powder and water was mixed manually to obtain a homogeneous paste. Trapped air was minimized by constant stirring and shaking. To minimize evaporation from the remoulded clays, the samples were mounted in a room with humidity around 90%. The clay slurries were carefully placed in the oedometer, and the initial porosity and bulk density of the samples were computed at room temperature and pressure conditions using the following relationships:

$$\phi_0 = \frac{V_0 - (m_s/\rho_s + m_k/\rho_k)}{V_0}, \quad (1)$$

$$\rho_b = \frac{m_s + m_k + m_w}{V_0}, \quad (2)$$

Table 1
Mineralogical composition determined by the X-ray diffraction spectroscopy (wt%)

Smectite	(wt%)	Kaolinite	(wt%)
Smectite	89	Kaolinite	81
Cristobalite	09	Illite/Mica	14
Quartz	02	Microcline	05

Table 2
Chemical composition determined by X-ray fluorescence spectroscopy analysis (wt%)

Constituents	Smectite (%)	Kaolinite (%)
SiO_2	71.51	47.67
Al_2O_3	14.28	35.06
Fe_2O_3	1.86	0.92
MnO	0.01	0.01
MgO	2.53	0.29
CaO	1.05	0.20
Na_2O	2.67	0.10
K_2O	0.27	2.87
TiO_2	0.20	0.06
P_2O_5	0.20	0.08
Loss of ignition	5.33	11.09
Total	99.91	98.35

where ϕ_0 and ρ_b are the initial porosity and bulk density, V_0 is the initial sample bulk volume computed from the initial specimen height and the oedometer area, m_s, m_k and m_w are the mass of the dry smectite, kaolinite and water in grams, and ρ_s and ρ_k are the specific densities of smectite and kaolinite grains. The measured grain densities 2.62 and 2.61 gm/cc, respectively, for smectite and kaolinite grains were used to calculate the initial porosity and bulk density for both dry and brine-saturated mixtures. The wet clay grain density could be lower than the laboratory measured dry grain density. Therefore, initial porosity and bulk density values for brine-saturated samples with assumed grain densities ranging from 1.9 to 2.6 gm/cc was checked. Changes in initial porosity and initial bulk density due to low grain density was found to be negligible and probably compensated after the first phase of rapid porosity reduction taking place at stress levels below 1 MPa.

2.2. High-stress oedometer

The compaction tests of dry clay mineral aggregate and brine-saturated clay slurries were performed by running constant rate-of-strain tests in the high-stress oedometer cell. A cross section of the apparatus is shown in Fig. 2. The oedometer area is 20 cm^2 and the cell height is 30 mm. The stainless steel oedometer cell has a highly polished inner surface. There will be some effects of side friction on the results, but they are considered to be small. The top cap and the base plate, both made of stainless steel, are provided with 2 mm thick porous disks connected to two drainage tubes to allow excess pore pressure to dissipate. The top cap diameter is 0.15–0.25 mm less than the inner oedometer ring diameter. Specimens were gently poured into the oedometer in order to obtain a high porosity as close as possible to the initial state of the porosity of clays at the time of deposition in sedimentary basins. A pore pressure sensor was used to monitor the pore pressure at the bottom of the specimen. The measured initial porosities of the dry samples were relatively low, but porosities of the brine-saturated samples

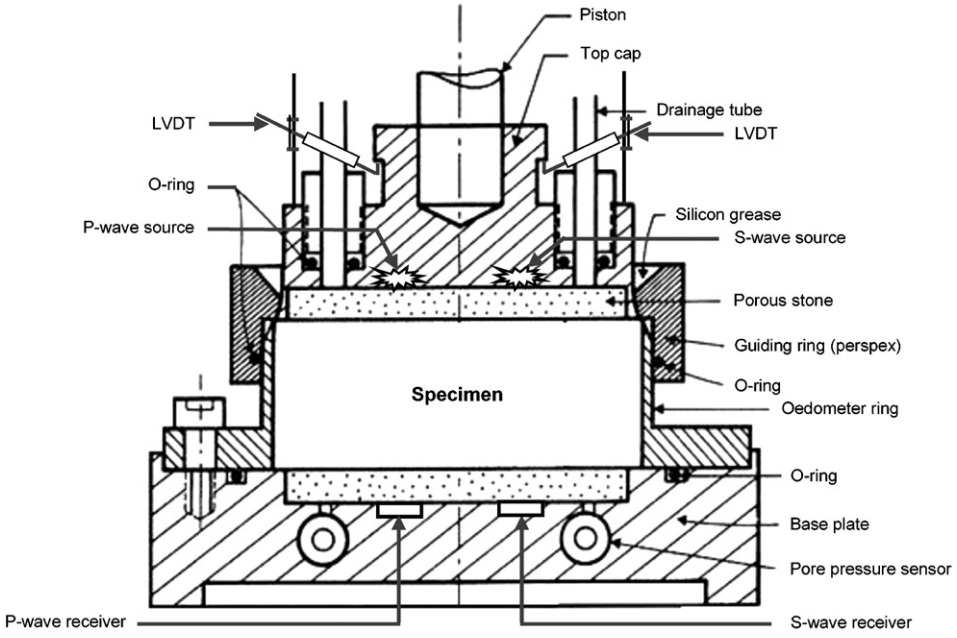

Fig. 2. A cross section of the high stress uniaxial oedometer cell.

mimic the porosity of natural muds usually found at the time of deposition. The mechanical compaction of dry specimens takes place much faster than for brine-saturated specimens. Brine-saturated samples were run under controlled pore pressure and drainage conditions. The vertical stress, pore pressure and vertical strains were measured continuously during the tests. The initial heights of the brine-saturated specimens were about 30 mm, but the final compressed heights in the range 8–10 mm.

During the brine-saturated tests, only a small excess pore pressure was found when compacting pure kaolinite under the constant rate of strain. The excess pore pressure increased with the amount of smectite in the mixture, and the highest pore pressure was observed in the pure smectite sample. The pore pressure was not allowed to exceed more than 10% of the vertical effective stress for all tests except for pure smectite where pore pressure was about 10–15% of the vertical effective stress at stresses higher than 10 MPa (Fig. 3a). The pure smectite compaction test took much longer time than for any other test (Fig. 3b). The sample height was precisely measured and monitored throughout the experiments using two linearly variable displacement transducers (LVDT). The vertical strain was measured as the specimen height change. This allowed computation of porosity and density changes as a function of stress. The volume decrease is equal to the volume of water or air expelled in wet and dry specimens, respectively, since the volume of the solid grains remains the same throughout the compaction process (Jones, 1944).

2.3. Acoustic velocity measurements

The pulse transmission technique (Birch, 1960) was used to measure compressional and shear wave velocities. To assure a more distinct first arrival for more reliable velocity estimation and to minimize the pulse-wave energy dissipation caused by diffraction, scattering, mode conversion and reflection phenomena, the following precautions were taken in the oedometer design and in the sample preparation:

(a) to avoid waveguide effect and geometric diffraction, the oedometer sample radius (r) was higher than the wavelength (λ) of the ultrasonic pulse ($r > \lambda$) (Anderson, 1961; Schreiber, 1973),
(b) to assure full ultrasonic pulse transmission through the sample from source to receiver, the final sample length/height (L_e) was greater than the pulse wave wavelength ($L_e/\lambda > 1$) (Kolsky, 1953),
(c) to avoid scattering of the ultrasonic wave by the pore fluid or grains in the samples, the transmitted pulse wave length was at least three times longer than the largest grain or pore (d_s) in the sample ($\lambda/d_s > 3$) (Plona and Tsang, 1978),
(d) to avoid cancellation of the direct first arrival amplitude by interference with waves reflected from the sample sidewalls, the sample length was at least five times less than the sample diameter ($L < 5d$).

The velocity measurements were performed throughout the compaction experiments as the effective stress was increased. The top cap and the base plate of the apparatus contain piezoelectric transducers (barium titanate), one set of which acts as the source and the other as the receiver (Fig. 2). Joint P- and S-transducers with functional resonant frequency 500 kHz was used to obtain high quality ultrasonic signals. The pulse traveled through the sample to the receiver transducer. The P- and S-wave

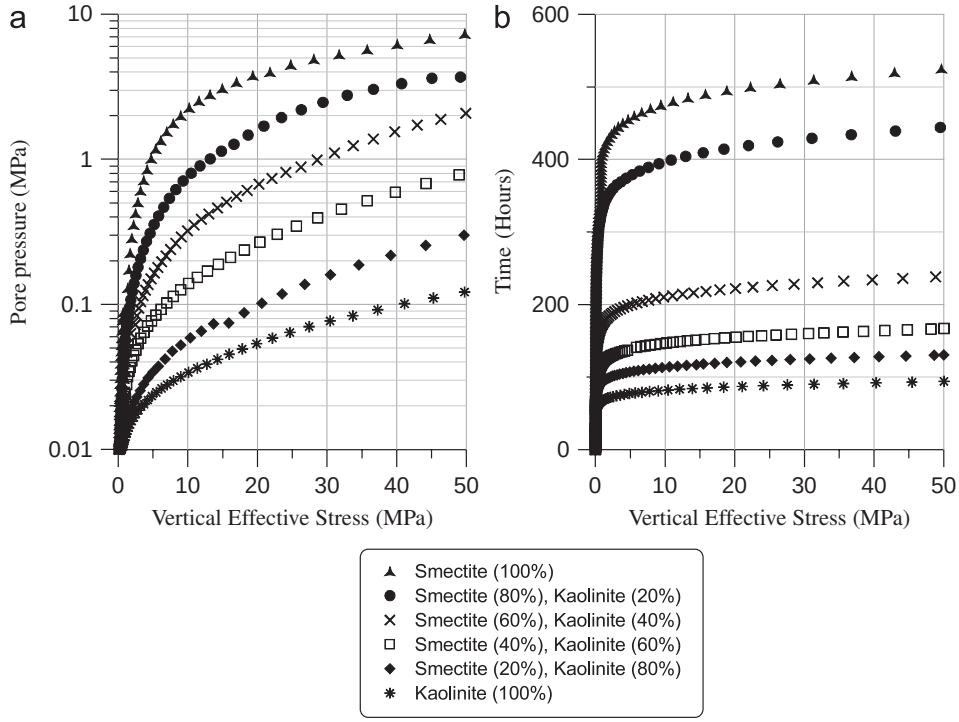

Fig. 3. (a) Plot of pore pressure (logarithmic scale) versus vertical effective stress for brine-saturated smectite and kaolinite mixtures. The pore pressure was always maintained and not allowed to exceed more than 10% of the vertical effective stress except for the pure smectite sample, where maximum pore pressure was about 15% at high stresses. (b) The run times (in hours) of laboratory compaction test versus vertical effective stress for the same clay samples. Tests were performed at room temperature. The applied maximum vertical effective stress was 50 MPa.

pulses received by the transducers were displayed on a digital oscilloscope and finally recorded by a computer for travel time analysis. The first arrival of the P-wave signal was easy to detect throughout the loading process, but the first arrival of the S-wave signal was difficult to distinguish until the vertical effective stress was above 5 MPa. This may be due to the influence of transit P-wave signals interrupting the S-wave signature at low stresses. Velocities were calculated using the following equation:

$$V = \frac{L}{T_s - T_o}, \tag{3}$$

where V is either P or S-wave velocity, L is the sample length, T_s and T_o are travel times with or without the sample in between the transmitter and receiver transducers, respectively.

3. Experimental results

3.1. Stress–compression relationships

The experimental compression results from dry and brine-saturated smectite, kaolinite and their mixtures expressed by the porosity–stress and density–stress curves can be found in Fig. 4a and b. The laboratory experiments show that kaolinitic clays compact much more than smectitic clays, and brine saturated clays are more compressible than the representative dry clay mixtures. This means that the compressibility of clay aggregates is not only a function of the physical strength of the clay particles as in sand, but also their interaction with the fluid phase. The laboratory measured initial porosities of dry and brine-saturated pure smectite samples were 67% and 81%, respectively, and reduced to 45% and 36% at 50 MPa vertical effectives stress. The dry and brine-saturated pure kaolinite samples had lower initial porosities, 63% and 71%, and reduced to 28% and 12%, respectively, at 50 MPa effective stress (Fig. 4a). The compaction curves for all 12 dry and brine-saturated clay mixtures fall within the range set by the compaction trends of brine-saturated kaolinite and dry pure smectite aggregates. The results show that clay compaction increase gradually with increasing kaolinite content in the mixture. Both dry and brine-saturated pure smectite retain 15–20 percentage points higher porosity along the whole stress path compared to pure kaolinite. The differences found between the two are relatively small at low stresses, but increase gradually with increasing effective stress. Generally, density increases fast during the early stages of compaction (0–10 MPa) before a slow steady increase takes place between 10 and 50 MPa. Kaolinite rich samples have higher bulk densities than smectite rich samples (Fig. 4b).

The porosity–stress and density–stress curves can be described by three stages based on the stress–compression behavior of dry and brine-saturated clay mixtures (Fig. 5a and b). The rate of porosity reduction in brine-saturated clays is much faster than in the dry clays at very low stresses between 0 and 1 MPa (Fig. 5b). On the other hand,

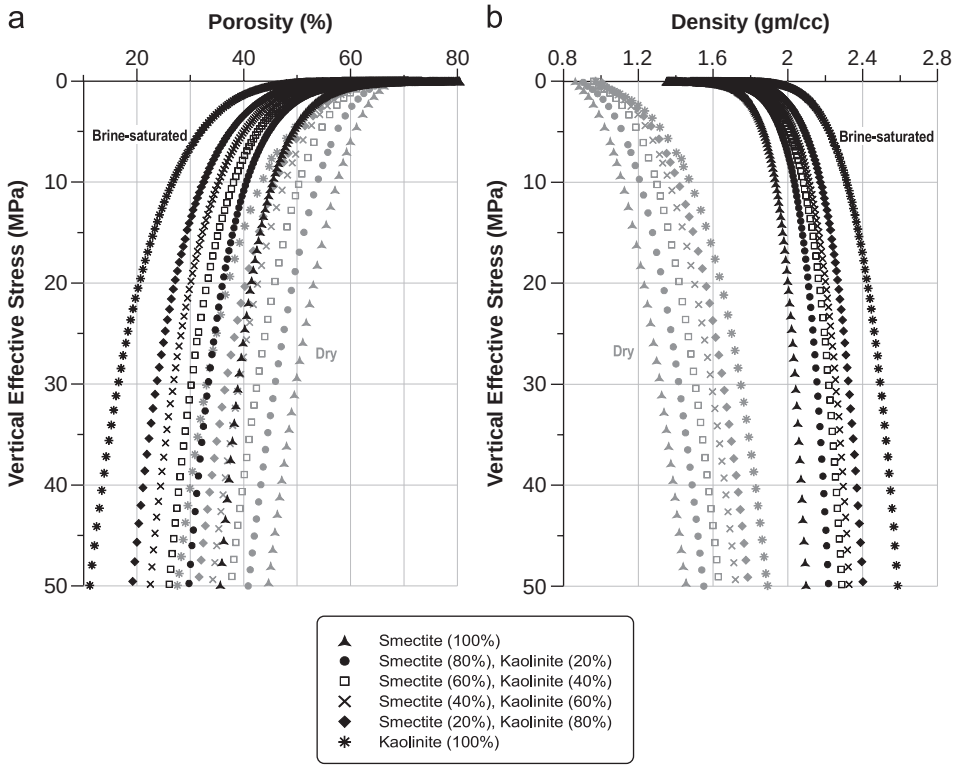

Fig. 4. Experimental mechanical compaction of dry (in gray) and brine-saturated (in black) smectite and kaolinite aggregates and their mixtures under uniaxial compression strain. Porosity reduction (a) and density variations (b) as a function of vertical effective stress up to 50 MPa are shown.

the maximum compaction rate occurs in dry clay mixtures at stress between 1 and 5 MPa (Fig. 5a). Above 5 MPa effective stress, the rate of porosity reduction accompanied by density increase are similar for both dry and wet clay mixtures. The rapid volume changes at low stresses found in wet clay mixtures are due to interstitial water loss before the clay particles come into contact with each other. Whereas in dry tests, volume changes takes place at low stresses due to initiation of reorientation and rearrangement of the solid particles. Particle rearrangements leading to a closer grain packing is the principle mechanism in the second stage of compaction of dry and brine-saturated clay mixtures. Only very gradual changes in porosity reduction are found in the third stage at stresses greater than 10 MPa when soft or smaller clay particles are forced into the interstices between larger or more competent grains as a function of high effective stress.

3.2. Stress–velocity–impedance relationships

The P- and S-wave velocities are also shown to be sensitive to clay composition in addition to effective stress. Brine-saturated clay mixtures have higher V_p than corresponding dry clay mixtures (Fig. 6a). At 1 MPa stress, kaolinite-rich (above 60% kaolinite) brine-saturated samples show lower V_p than brine velocity (~1500 m/s). V_p of pure smectite aggregates is higher in the dry and lower in brine-saturated state than in the pure kaolinite aggregates. A sharp V_p increase is observed at low stresses (0–20 MPa) for all dry and brine-saturated clay mixtures. This corresponds to the rapid porosity reduction found at low stresses. The increment of V_p is more or less consistent for all clay mixtures from 20 to 50 MPa. The maximum difference of V_p is observed between dry and brine-saturated clay aggregates at low stresses. The difference tends to be smaller with increasing effective stress (Fig. 6a). The brine-saturated sample containing 40% smectite and 60% kaolinite shows maximum V_p compared to all other smectite–kaolinite mixtures along the whole stress path. This may possibly be interpreted as best packing of two end clay members at this weight fraction.

V_s, however, exhibit the opposite behavior of the V_p. In particular, as the V_s found in the brine-saturated samples are lower than in the corresponding dry samples (Fig. 6b). The V_s measurements were indistinct at low stresses (less than 5 MPa) possibly due to the softness of the specimens. The V_s presented for all clay mixtures below 5 MPa are calculated from an extrapolation of the best fit line for the particular sample. The V_s increase is almost identical for all dry clay aggregates, but it varies significantly in the brine-saturated case. The difference in V_s between dry and brine-saturated samples increases with increasing vertical effective stress. There is a small difference in V_s between pure smectite and kaolinite aggregates in the dry state, but in brine-saturated state the difference between them is substantial. Kaolinite-rich samples have the highest V_s, and the smectite-rich samples have the lowest V_s in the brine-saturated condition (Fig. 6b).

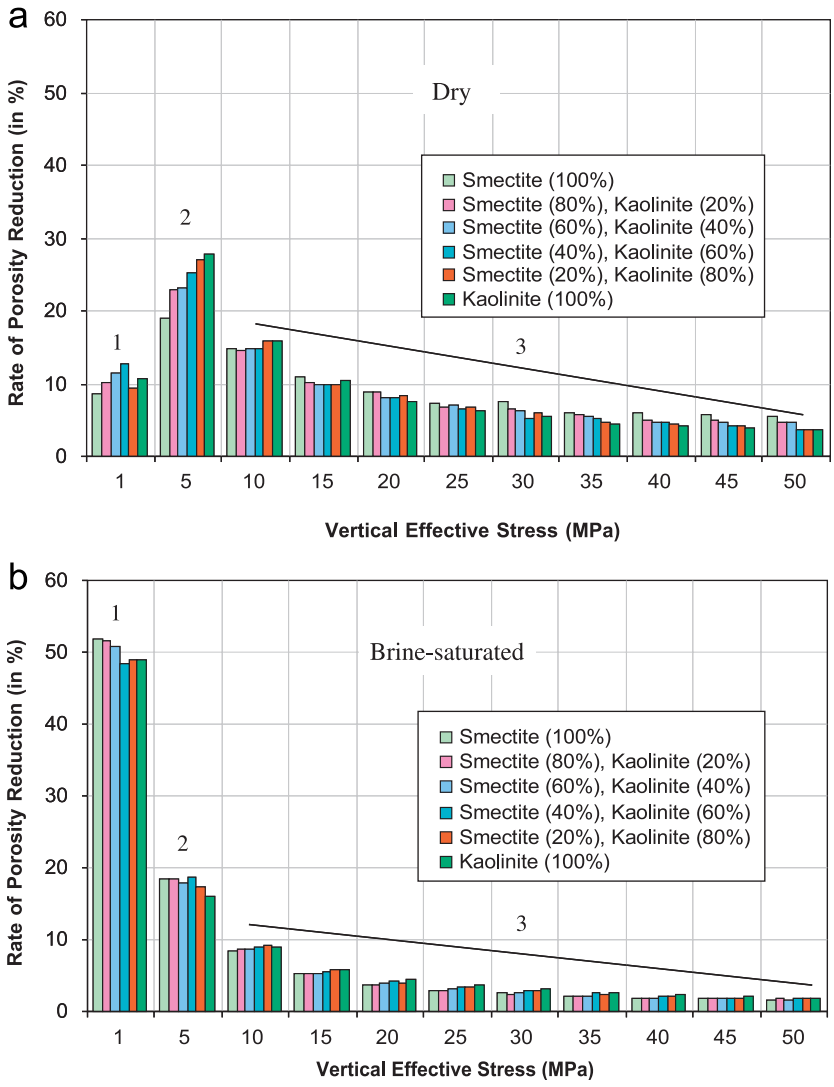

Fig. 5. The rate of porosity reduction (in %) of dry (a) and brine-saturated (b) smectite–kaolinite mixtures as a function of vertical effective stress is shown. The porosity reduction rate is calculated by normalizing the porosity lost deriving the compaction to 100%. The rate of porosity reduction is divided into 3-stages (marked by 1, 2 and 3) based on the stress–compression behavior found for the clay mixtures. The porosity decrease is highest between 0 and 1 MPa (50%) corresponding to about 100 m burial depth of normally consolidated basin under hydrostatic pore pressure.

Impedance, the product of density and velocity, is the important property for determining the amount of energy reflected when elastic waves pass one medium to another. Fig. 6c and d are the cross plots of calculated P- and S-impedances (I_p and I_s) versus effective stress for dry and brine-saturated clay mixtures. More systematic and distinct differences in P- and S-impedances versus effective stress are found in the dry and brine-saturated clays than in the P- and S-wave velocity plots in Fig. 6a and b. The I_p differences are large between dry and brine-saturated clay mixtures, while the differences in I_s are relatively small. Smectite aggregates shows low I_p and I_s compared to kaolinite in both dry and brine-saturated conditions. At low stresses, the differences in I_p and I_s are relatively small for all clay mixtures in dry and brine-saturated clays, respectively, but the differences increase significantly with increasing vertical effective stress.

3.3. Velocity ratio with respect to stress, density and P-wave velocity

The velocity ratio has significant importance in reflection seismics and formation evaluation. Pickett (1963) promoted its use as a lithology indicator. The velocity ratios of dry and brine-saturated clay mixtures as function of vertical effective stress are shown in Fig. 7a. In brine-saturated clay mixtures, velocity ratios are much higher than in the corresponding dry clay mixtures. The V_p/V_s ratios of dry clay aggregates converge with increasing stress, while the brine-saturated clays maintain the differences in V_p/V_s ratio with increasing effective stress. A significant drop of the V_p/V_s ratios of smectite and kaolinite aggregates are recorded in brine-saturated state at effective stresses between 1 and 50 MPa. The V_p/V_s ratio of dry smectite-kaolinite mixtures is more or less unaffected

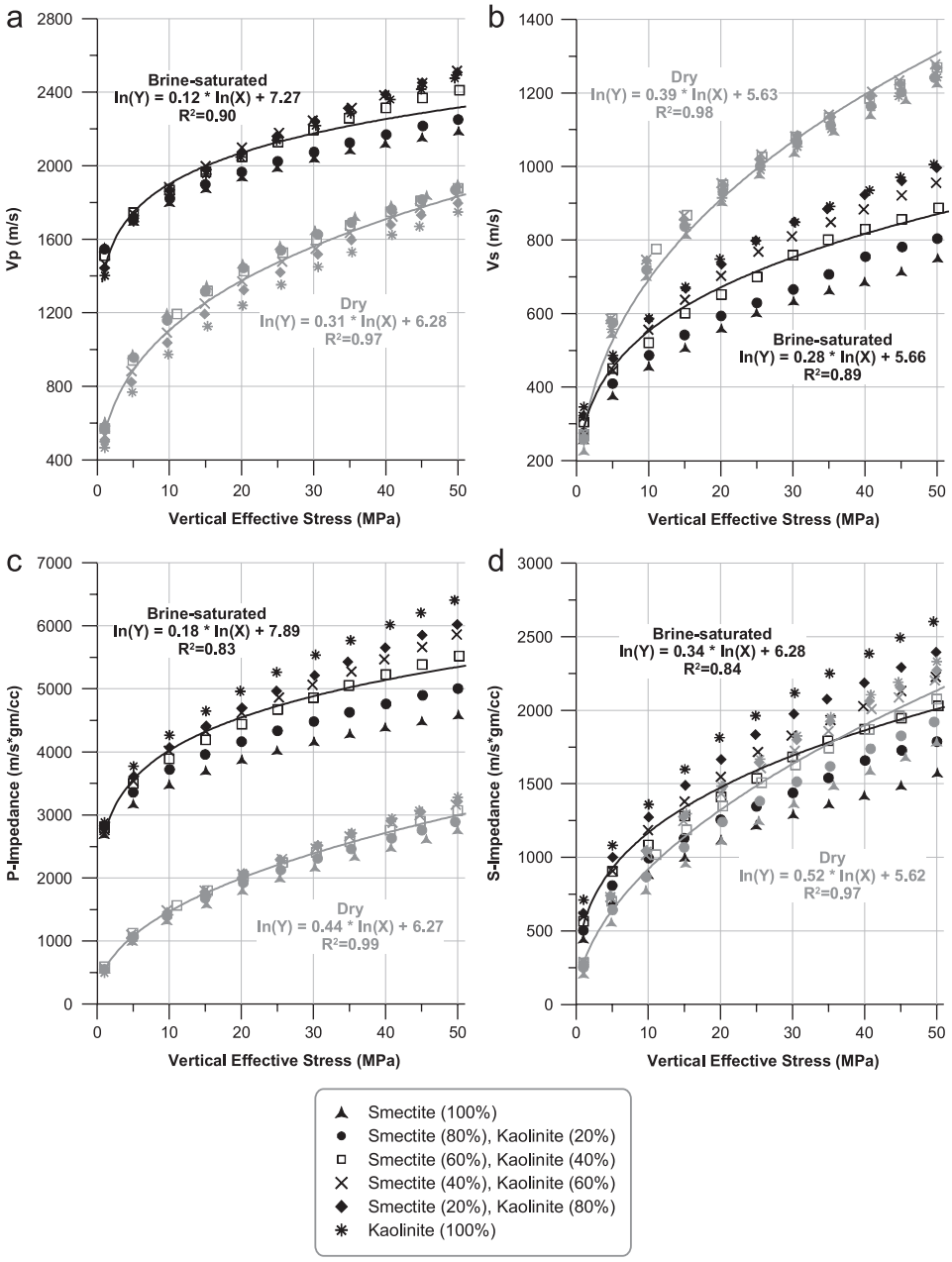

Fig. 6. Cross plots of P-wave velocity (a), S-wave velocity (b), P-impedance (c), and S-impedance (d) versus the vertical effective stress for dry (in gray) and brine-saturated (in black) clay mixtures. Lines show least squares fits to the data. Equations for best fit lines and the correlation co-efficient (R^2) are also shown with the plots.

by the increasing effective stress with an exception at low stresses between 1 and 5 MPa (Fig. 7a).

The V_p/V_s versus density cross plot presented in Fig. 7b shows that dry clays are little affected in terms of density variations accompanied by effective stress, while the V_p/V_s ratio in the brine-saturated case shows a sharp decrease with increasing density. The velocity ratios and their differences within all clay mixtures are larger at lower density conditions, and the differences reduce significantly at high density level. This implies that specimens having a similar degree of consolidation, the lower the density, the larger the V_p/V_s ratios will be. As far as V_p/V_s is concerned, it is difficult to determine whether the increase in the V_p/V_s ratio is caused by an increase in porosity or by a decrease in compaction.

Fig. 7c shows the V_p/V_s ratio as a function of P-wave velocity. This plot shows the strong V_p/V_s ratio versus V_p relation for brine-saturated clays. Much higher V_p/V_s ratios are observed for brine-saturated clays than dry clays, and the differences among individual clay aggregates also vary with respect to V_p. As expected, the V_p/V_s ratio is highest for smectitic aggregates and lowest for kaolinitic aggregates in both dry and brine-saturated conditions. V_p and V_s are affected by the effective stress in a similar

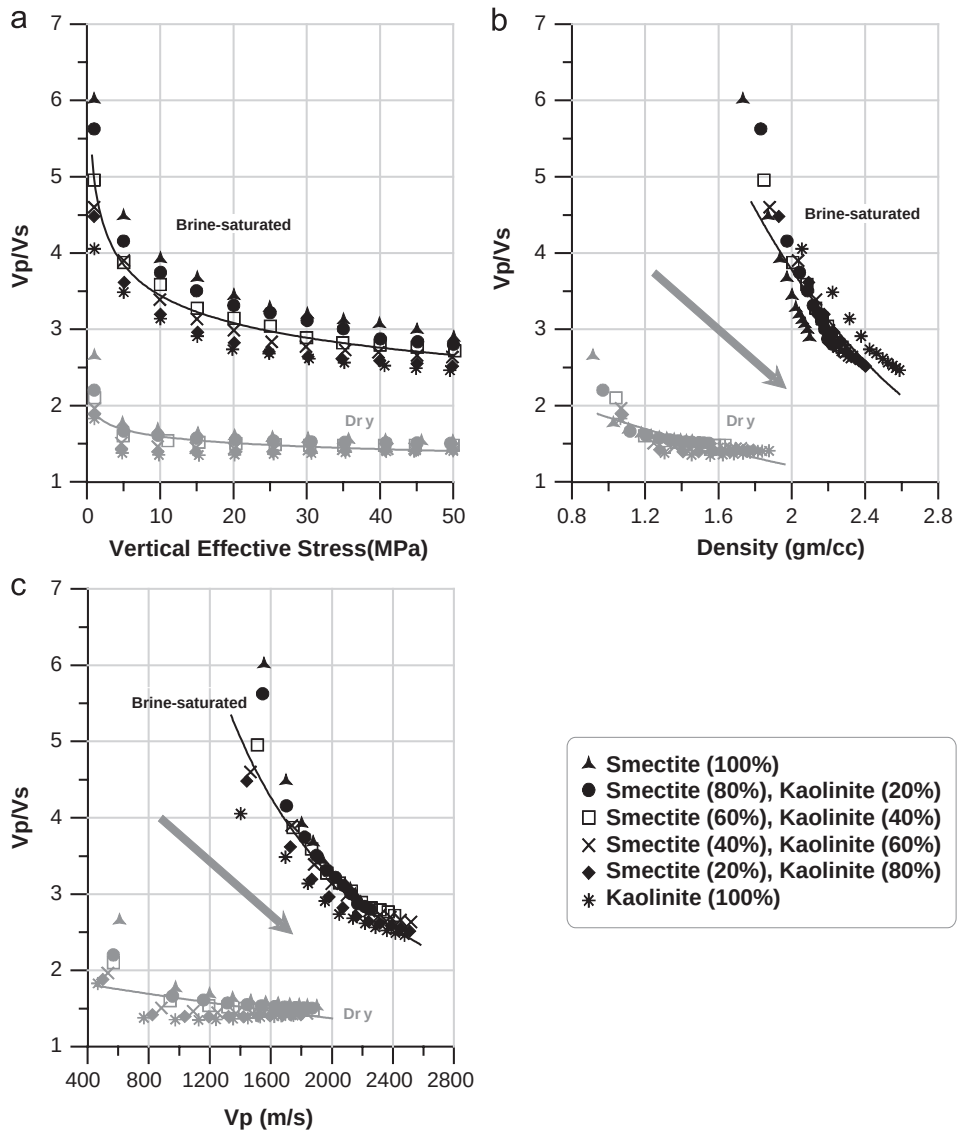

Fig. 7. Cross plots of V_p/V_s ratio of two end members clays and their mixtures as functions of vertical effective stress (a), porosity (b), and V_p (c) at dry (in gray) and brine-saturated (in black) states. Lines show least squares fits to the data and the arrow shows increasing direction of vertical effective stress.

manner. While fluid content affect only on V_p and insensitive to V_s. So, the V_p/V_s ratio in porous media is primarily determined by the fluid content.

3.4. Derivation of material parameters from density and wave velocities

The measured V_p, V_s and densities of smectite-kaolinite mixtures can be used to calculate equivalent elastic parameters. The following relations between the elastic parameters, density and velocities are used in the calculations:

$$\mu = \rho V_s^2, \tag{4}$$

$$E = \rho V_s^2((3V_p^2 - 4V_s^2)/(V_p^2 - V_s^2)), \tag{5}$$

$$v = (E - 2\mu)/2\mu, \tag{6}$$

$$K = E/(3(1 - 2v)), \tag{7}$$

$$\lambda = K - 2\mu/3, \tag{8}$$

where μ is shear modulus (GPa); E is Young's modulus (GPa); v is Poisson's ratio; K is bulk modulus (GPa); and λ is Lame's constant. Fig. 8 shows calculated elastic moduli for dry and brine-saturated aggregates of smectite and kaolinite mixtures as a function of vertical effective stress. The elastic moduli versus effective stress plots show that brine-saturated clay aggregates have distinct and much higher values of K (Fig. 8a), v (Fig. 8d) and λ (Fig. 8e) compared to dry clay mixtures. The μ and E of dry and brine-saturated samples fall within a close range with exception of two brine-saturated samples. The brine-saturated aggregates of smectite (100%), and smectite (80%) and kaolinite (20%) show relatively lower μ and E than the other clays. The brine-saturated pure

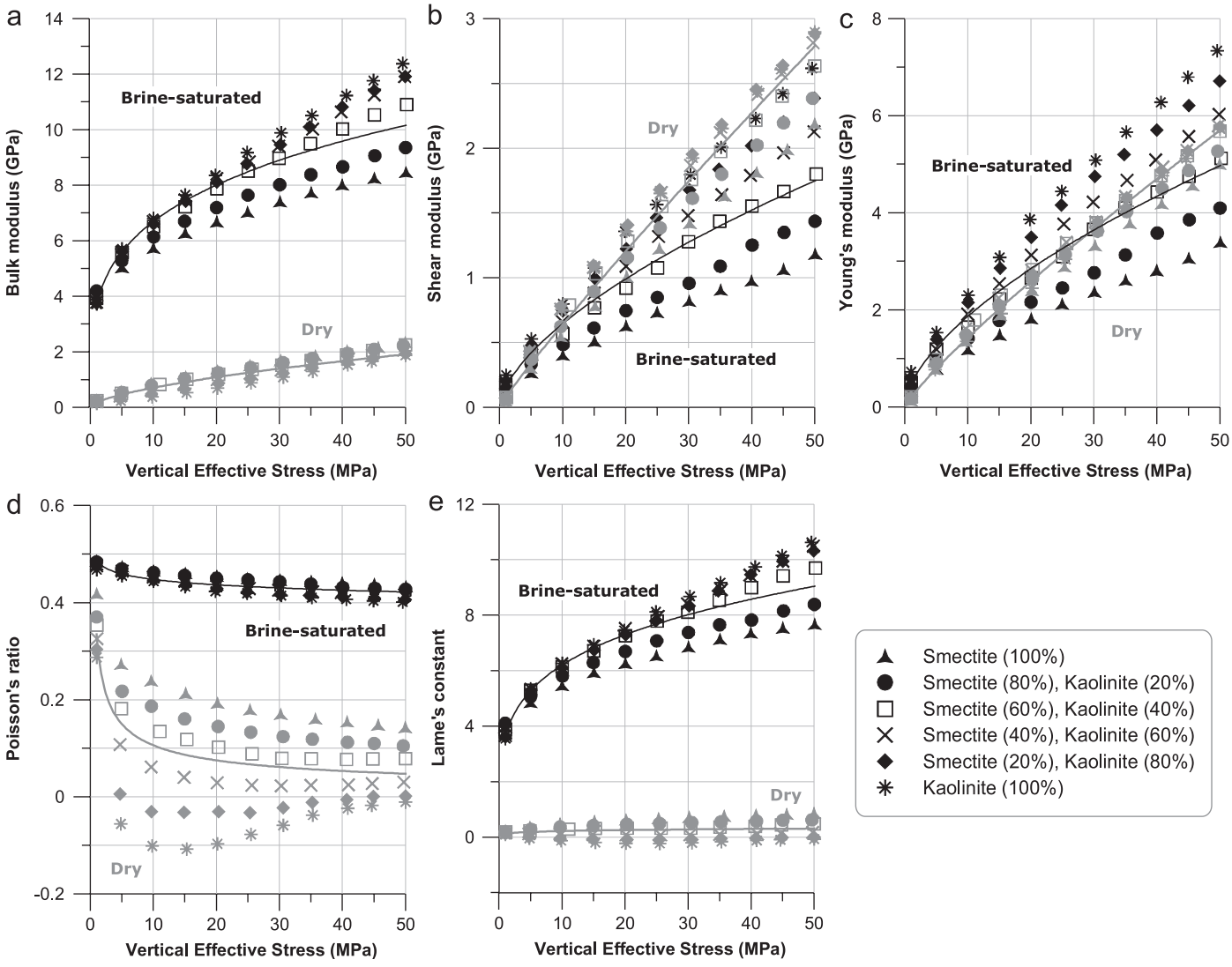

Fig. 8. Vertical effective stress–moduli relationships for dry (in gray) and brine-saturated (in black) smectite-kaolinite mixtures. Bulk (a), shear (b) and Young's modulus (c), as a function of vertical effective stress are shown in the top row. The relationships between Poisson's ratio, (d) and Lame's constant, (e) with respect to the vertical effective stress are shown in the bottom row. Least squares fits to the data are shown by the gray (dry clays) and black (brine-saturated clays) lines.

kaolinite (100%) and the kaolinite (80%) and smectite (20%) mixture have highest E than rest of clay mixtures (Fig. 8c).

K and λ are nearly identical for all dry clay mixtures (Fig. 8a and e). The increase of K and λ recorded in the dry clay aggregates as a function of stress is much smaller than for the respective brine-saturated aggregates. The ν of dry clay mixtures are significantly lower and differ much more from each other than for the brine-saturated clays. The clay aggregates in brine-saturated condition show little difference in ν for all stresses. Negative values of ν and λ are recorded for aggregates for pure kaolinite (100%) and kaolinite (80%) and smectite (20%) at stresses between 5 and 50 MPa (Fig. 8d and e). The differences of λ of all brine-saturated clay mixtures increase with increasing vertical effective stress.

4. Discussion

4.1. Interpretation of experimental compaction of clays

The present experimental compaction data provide information about how clay samples with known composition respond to effective stresses similar to those experienced under natural burial conditions. The compaction of clays and muds is a complex process and involves the mechanical strength of the grains, grain size and specific surface area, as well as surface charges (Skempton, 1953; Meade, 1964; Djeran et al., 1998; Yang and Aplin, 1998; Grabowska, 2003). The compressibility of clays and muds is also a function of interactions between the solid phase and the fluid phase (Bolt, 1956; Mitchell, 1960; Engelhardt and Gaida, 1963; Meade, 1963; Wijeyesekera and DeFreitas,

1976). Compaction behavior is therefore quite different in dry clays compared to wet. The laboratory experiments show that brine saturated clays are much more compressible than dry clays as brine may soften and lubricate the matrix material and reduce the internal friction between clay particles. The relative compressibility found in dry and brine-saturated clay mixtures between kaolinite and smectite remains the same (Fig. 4). Dry clay mixtures compact due to matrix inelasticity, including frictional dissipation from relative motion at grain boundaries. Brine saturated clays compact by elimination of pore space subsequent to expulsion of interstitial water.

The laboratory investigation also demonstrates that the pure smectite aggregates is least compressible and the pure kaolinite aggregates is most compressible both in dry and brine-saturated states. This can be interpreted as a mechanical effect. The very fine-grained smectite distributes the total stress over a very large number of grain contacts so that the force per contact is low compared to that in coarse-grained kaolinite. A similar effect was found for compacting sandstones where well sorted fine grained sand was found to be much less compressible than coarse grained sands (Chuhan et al., 2002, 2003). Controlled experiments like in the present study using end member clays (smectite and kaolinite) with respect to grain size, surface area and ion exchange capacity, reveal the range in clay compaction behavior. Other clay minerals like chlorite and illite are intermediate between smectite and kaolinite with respect to the above mentioned properties and are expected to compact in-between smectite and kaolinite (Chilingar and Knight, 1960; Meade, 1963; Meade, 1966; Rieke and Chilingarian, 1974). A marked decrease in porosity is observed in the laboratory at very low stresses (<1 MPa) for all brine-saturated clay mixtures (Fig. 5b). Brine-saturated samples containing more than 60% smectite are more susceptible to compaction at low stresses (1 MPa) compare to rest of clay mixtures. For dry clays the opposite behavior is observed where kaolinite rich clays are more compressible at stresses around 5 MPa that equivalents to maximum compaction stress of dry clay mixtures (Fig. 5a).

In addition, the present experiment shows that a pure kaolinitic rock is expected to preserve 20% porosity at 20 MPa effective stress corresponding to about 2 km burial depth under hydrostatic pore fluid pressure. This is less than half the porosity that will remain in a pure smectitic rock at the same stress or depth of burial (Fig. 4). The dependency of clay compaction on lithology, initial thickness, maximum effective stress, rate of loading, decomposition of the organic material, and recrystallization and decomposition of clay minerals is also stated by Rieke and Chilingarian (1974). Meade (1966) listed additional factors influencing the water content of clayey sediments subjected to stress are particle size, type of clay minerals, absorbed cations, interstitial electrolyte solutions, acidity and temperature. The experimental data presented here are only valid for the mechanical part of the compaction in sedimentary basins. The physical properties of natural samples are strongly influenced by chemical compaction and early formed carbonate cement may cause very high modulus and velocities even at shallow depth. Smectite compacts mechanically until it dissolves and is replaced by mixed layer minerals and illite at temperatures between 80 and 110 °C releasing silica which is precipitated as quartz cement (Bjørlykke et al., 1986; Bjørlykke, 1999).

4.2. Comparison of experimental and published porosity–stress/depth trends

A comparison between porosity–stress relationships of clays performed in this study and published porosity–depth trends found for argillaceous sediments is shown in Fig. 9. A linear relationship has been used between effective stress and depth (1 MPa effective stress is equivalent to 100 m depth of burial with hydrostatic pore pressure) for conversion of the test results to burial depth. A wide range of initial porosities are found in published porosity–depth trends (Fig. 1). Some published studies dealt with sediments with initial porosity lower than 60% (Athy, 1930; Hedberg, 1936; Weller, 1959; Proshlyakov, 1960; Vassoevich, 1960; Durmishyan, 1974; Baldwin and Butler, 1985; Fowler et al., 1985; Goulty, 1998). Laboratory investigations show that initial clay porosity reduces dramatically by adding sand and silt particles explaining the low porosities reported in the above mentioned studies.

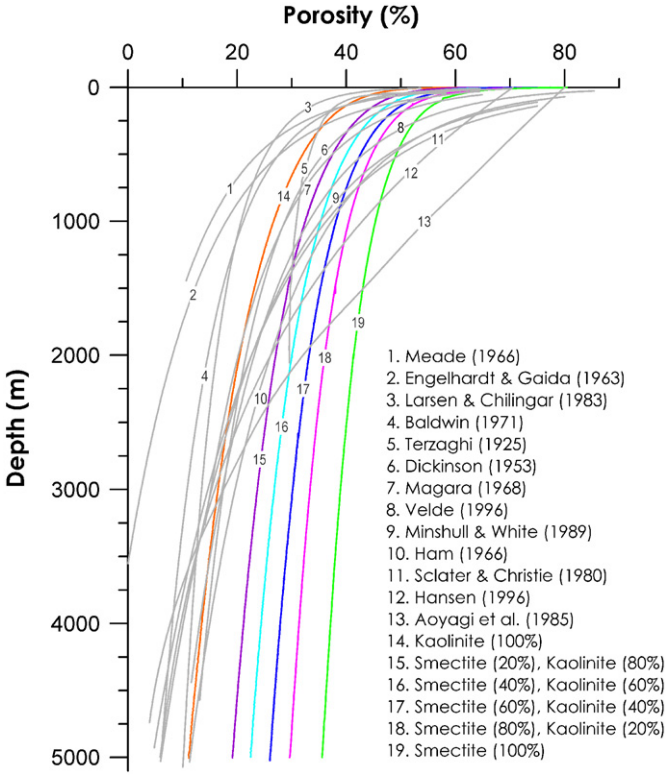

Fig. 9. A comparison of published porosity–depth trends for shales and argillaceous sediments (gray curves) and experimentally compacted curves of brine-saturated smectite, kaolinite and their mixtures (colour curves).

The present laboratory investigation shows that initial porosities of brine-saturated clay mixtures vary from 71% to 81% depending on weight fraction of clay minerals. Smectite-rich samples absorb more water than kaolinite rich samples and have therefore retained more initial porosity. These differences are mainly due to the different grain-size distributions and to the differences in the specific surface areas of smectite and kaolinite. The measured values are comparable to high initial clay and mud porosities ranging between 70% and 90% reported by many authors (Dickinson, 1953; Hamilton, 1976b; Sclater and Christie, 1980; Minshull and White, 1989; Velde, 1996). Thus the comparison shown in Fig. 9 includes only published porosity–depth trends with initial porosity above 70%. The measured compaction trends of dry smectite–kaolinite mixtures are also excluded from this comparison.

Fig. 9 shows a comparison of selected published porosity–depth curves (1–13) and our experimental curves (14–19) for brine-saturated smectite and kaolinite mixtures. The published curves illustrate a wide range of compaction trends for argillaceous sediments. The publish trends differ most at shallow burial depths. The difference reduces significantly below 2000 m burial depth with curves 1 and 2 as exceptions. None of the of published compaction curves match each other or the experimental curves from this study with the exceptions of the shallow part of curves 3, 4 and 5 and experimental curve 14. The discrepancies may be due to differences in lithologies, pore pressure and/or diagenetic history. A marked difference is found at depths below 2000 m between the laboratory measurements and the published curves. This depth could, based on the published curves, be interpreted as the starting depth for chemical compaction (Bjørlykke and Aagaard, 1992; Bjørkum et al., 1998; Bjørlykke, 1999; Storvoll et al., 2005). The experiments also show that sediment porosity is only marginally influenced by mechanical compaction at depth greater than 2000 m. If chemical compaction takes place, mechanical compaction will be negligible below this depth.

From Fig. 9 it is apparent that porosity-depth relations in argillaceous sediments cannot be satisfactorily generalized for the whole depth range and must be divided into stages in which certain processes dominate. The porosity–depth relations at shallow depth indicate that mechanical compaction in general follows a well-defined law dependent on starting material and other post depositional factor. There is no single, simple curve that fit all these data using exponential or log functions. Comparison of laboratory compaction curves and natural compaction trends should therefore be treated very carefully. Laboratory compaction curves have obvious limitations but can be very useful during compaction analyses.

4.3. Relationship of velocity, impedance and elastic moduli to effective stress and porosity

Laboratory determinations demonstrate that velocities, impedances and elastic moduli of clay aggregates vary significantly with clay mineralogy and pore fluid. The distinct differences in velocities, impedances and elastic moduli of corresponding dry and brine-saturated clay mixtures with respect to stress and porosity support their strong dependencies on clay mineralogy as well as pore-filling substances (Figs. 6, 8, 10 and 11). V_p is higher when clay mixtures are saturated with brine than when they are dry. For S-waves the behavior is opposite. V_s is higher in the dry case than in the brine-saturated case (Fig. 6a and b). The acoustic velocities in individual clay mixture also differ to some degree from one sample to another. In the dry state, this can be explained by the degree of anisotropy of the clay matrix and framework of clay grains. The dependence of V_p and V_s on rock framework, porosity and pore aspect ratio is shown in the literature (Biot, 1956; Kuster and Toksoz, 1974b; Cheng and Toksoz, 1976). Experimental results show that porosity has less influence on V_p, I_s, μ and E but has strong influence on V_s, V_p/V_s ratio, I_p, K, ν, and λ (Figs. 10 and 11). A comparison of physical properties of dry and brine-saturated clay mixtures with respect to vertical effective stress and porosity is shown in Table 3. A scatter of V_s in the brine-saturated state compared to dry state indicates the sensitivity of clay minerals to brine as the S-wave itself is not influenced by water (Fig. 6b). The lowest V_s value is observed in pure smectite aggregates whereas the highest value is found in pure kaolinite aggregates as a function of stress. Our measured V_p in brine-saturated clays at low stresses agree reasonably well with Hamilton's (1976a) and Hamilton and Bachman's (1982) measurement. They also found V_p in shallow unlithified, marine clays to be lower than the velocity in the brine alone. They also concluded that all marine sediments posses enough rigidity to allow transmission of shear waves even at shallow depth.

The dry and brine-saturated clay mixtures show two distinct developments in the plot of V_p versus V_s, I_p versus I_s, and bulk versus shear modulus (Fig. 12). The data are scattered within the range of pure kaolinite and pure smectite aggregates, suggesting that V_p and V_s are principally controlled by mineralogy. Adding water increases V_p and decrease V_s for clay mixtures. V_s, I_s and μ are linearly related to V_p, I_p and K for both dry and brine-saturated mixtures. The V_p/V_s, I_p/I_s and bulk/shear modulus ratio are very sensitive to pore filling substances. Measurements of these parameters in specimens saturated with oil will fall within the limits of dry and brine-saturated states (Toksoz et al., 1976; Pedersen et al., 1996; Benson and Wu, 1999). The measured V_p versus V_s of brine-saturated clays and the empirical V_p versus V_s relations for shales and mudstones show that the mudrock line (Castagna et al., 1985) marked by 1 in Fig. 12a tends to overestimate and the empirical equations by Han (1986) (line 2 in Fig. 12a) and Castagna et al. (1993) (line 3 in Fig. 12a) underestimate the measured V_p/V_s ratio. A strong stress and porosity influence on the V_p/V_s ratio is observed in brine-saturated clay mixtures, but the influence is negligible for dry mixtures (Figs. 7a and 10c). The effect

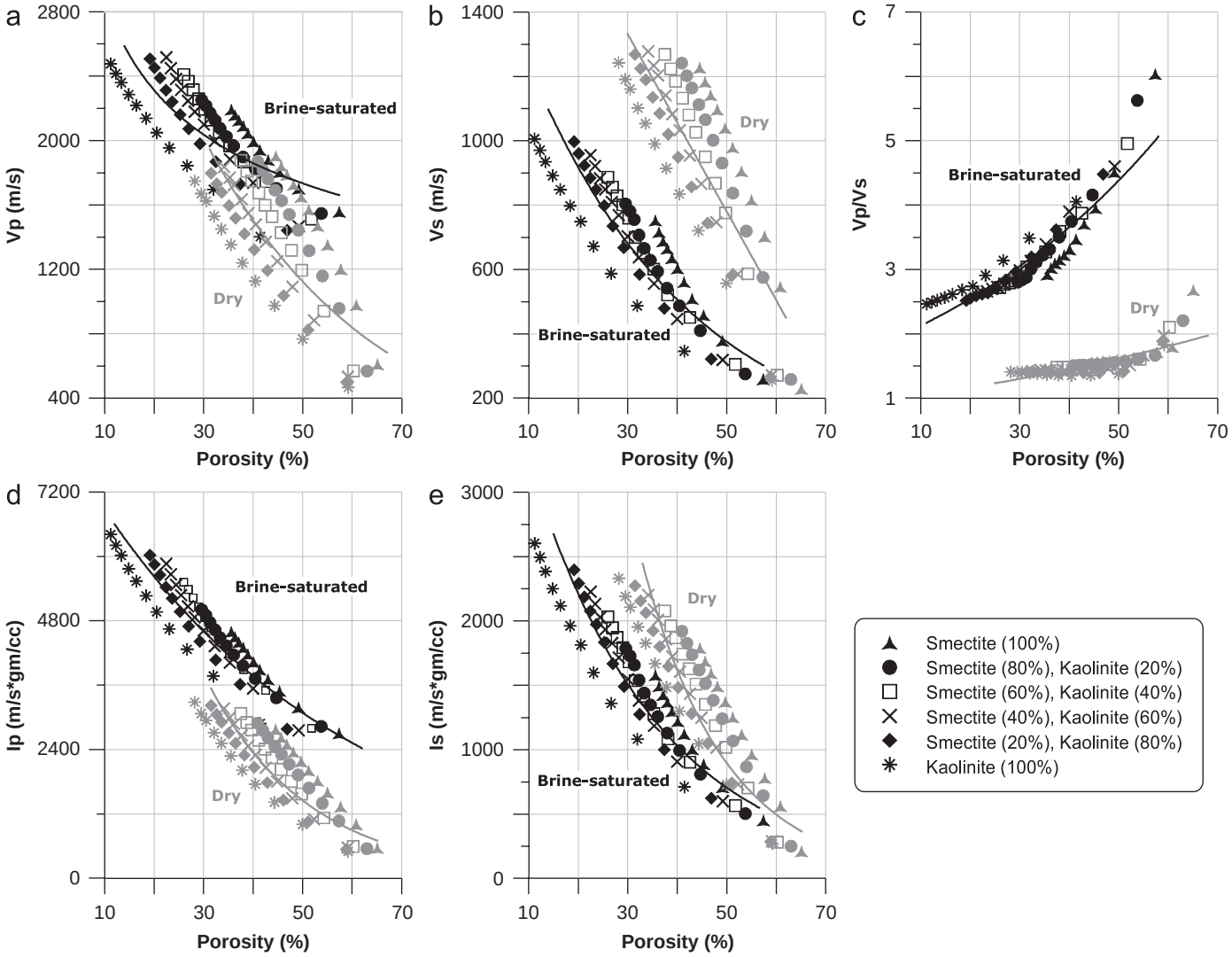

Fig. 10. Relationships between V_p (a), V_s (b), V_p/V_s ratio (c), I_p (d) and I_s (e) versus porosity for dry (in gray) and brine-saturated (in black) clay mixtures as a function of vertical effective stress. Least squares fits to the data are shown by the gray (dry clays) and black (brine-saturated clays) lines.

of vertical effective stress on velocity ratio for brine-saturated clays is much larger than for dry clay mixtures. The large variation in the V_p/V_s ratio shows the profound influence of smectite on velocity. The amount of smectite in clays control the V_s more than V_p, so increasing smectite content increases the V_p/V_s in clays. The effect of clay on the V_p/V_s ratio is also described in the literature where increasing clay content shows increase in the V_p/V_s ratio (Blangy et al., 1993; Lee, 2003). The present experiments show that an increase in the V_p/V_s ratio is a function of a decrease in effective stress (Fig. 7a), a decrease in density (Fig. 7b) or an increase in porosity (Fig. 10c) or a combination of the three.

The observed V_p and V_s for clay mixtures agree qualitatively well with that predicted by Biot's (1956) theory, except the S-wave velocities at stresses lower than 1 MPa. The S-wave velocities are higher in some wet clay samples compared to dry samples at very low stresses (about 1 MPa) (Fig. 6b). This behavior contrast Biot's theory, which predicts that S-wave velocities in dry rocks will be greater than in fluid saturated rocks at the same confining stress. A model which accounts quantitatively for the behavior that we observed at low stresses for S-wave, has been developed by Kuster (1977). According to the model, saturation of flat low aspect ratio cracks (porosity) increase the stiffness significantly, whereas saturation of spherical pores hardly affects the elastic moduli. For brine-saturated samples, the velocity variations of smectite and kaolinite at low stresses might be influenced by flat low aspect ratio pores.

Elastic constants provide further insight into the physical properties of composite granular media. Recent developments in exploration geophysics have emphasized the need for better understanding of the elastic parameters of clay minerals. The elastic parameters found in the literature for clay minerals are inconsistent and vary within a wide range (Katahara, 1996; Wang et al., 2001; Prasad et al., 2002; Vanorio et al., 2003), mainly because of the difficulty

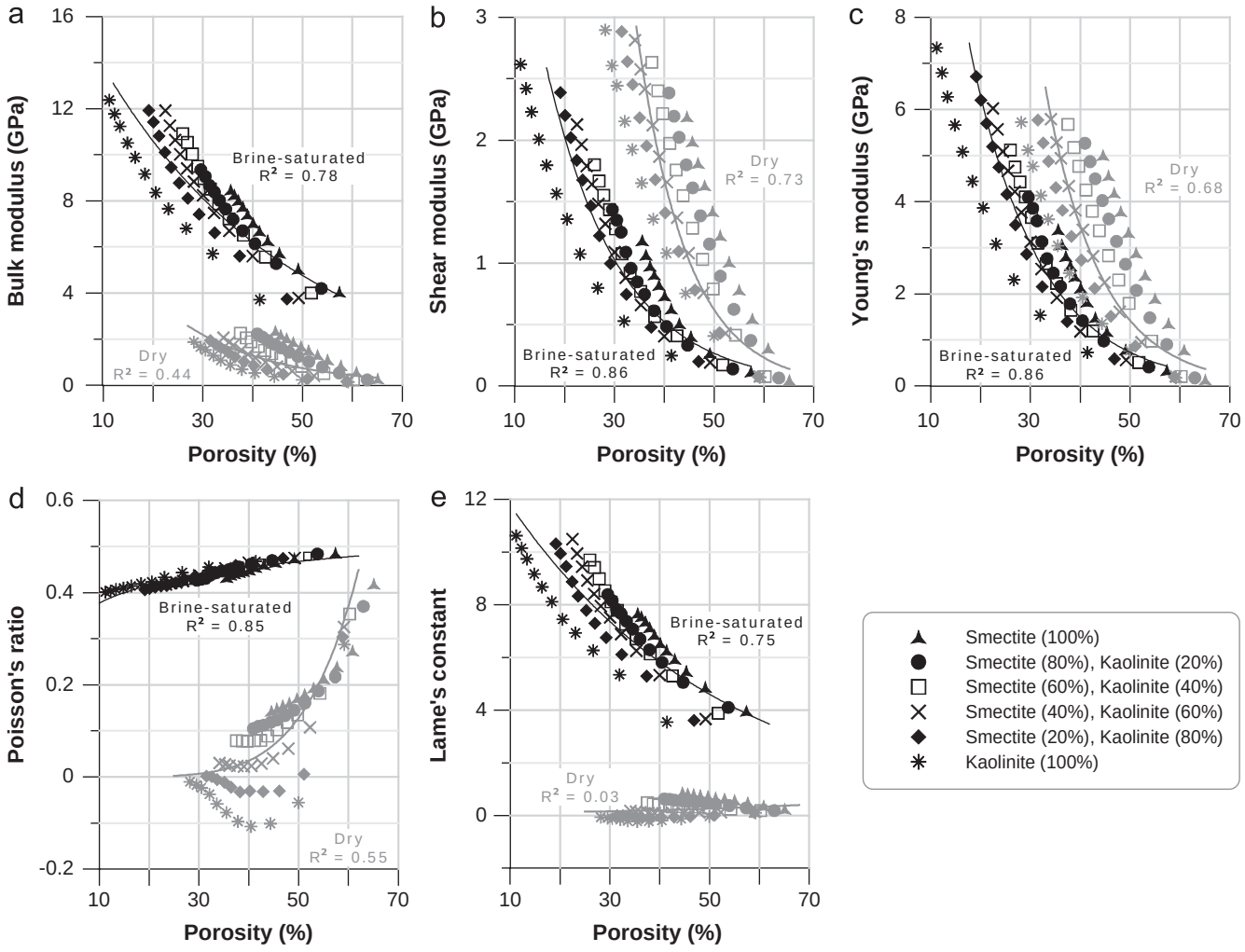

Fig. 11. Porosity–moduli relationships for dry (in gray) and brine-saturated (in black) smectite and kaolinite mixtures. Cross plots of bulk (a), shear (b), and Young's modulus (c), versus porosity are shown in the top row. The relationships between Poisson's ratio (d), and Lame's constant (e) to porosity are shown in the bottom row. Black and gray lines represent least squares fits to the data.

presented by their intrinsic properties. Our experimental results show higher elastic constants for smectite aggregates than for kaolinite for any given porosity value with an exception of Poisson's ratio in the brine-saturated state where little difference is found (Fig. 11). The relationships of porosity and elastic parameters are more systematic for dry clays where elastic parameters increase in a regular manner with increasing smectite content in the mixture. Smectitic clays have the lowest K, μ and E for a given effective stress due to low smectite compressibility (Fig. 8a–c).

Fig. 13a shows a comparison of V_p versus porosity of brine-saturated smectite-kaolinite mixtures (this study) and three other brine-saturated sediments, ranging from ocean bottom suspensions to consolidated clay-bearing sandstones (Hamilton, 1956; Han, 1986; Yin, 1992). The Reuss bound (Reuss, 1929), computed for mixtures of quartz and water, is also shown for comparison. Data measured at low effective stresses (<5 MPa) in smectite–kaolinite mixtures (within red ellipse) correspond well with ocean bottom suspension sediments (Hamilton, 1956). Upon increasing effective stress, that gives the strength of smectite–kaolinite mixtures, data (within cyan ellipse) moves off from the Reuss bound and fall on top of Yin's (1992) sand–clay data with an exception of pure kaolinite aggregates. It shows even lower value than the Reuss bound (Fig. 13a). As expected, high stress data of smectite–kaolinite mixtures fall far off from the clay-bearing sandstones (Han, 1986) as mudstones are less stiffer than sandstones. Fig. 13b shows another comparison of bulk modulus and porosity of our laboratory measurements and data from barine-saturated kaolinite (Yin, 1992) and kaolinite water suspension (Vanorio et al., 2003). The Hashin–Shtrikman lower bounds (HS^-) of the bulk modulus of a water–clay mixture are also compared with the data (Hashin and Shtrikman, 1963). The calculation of HS^- were made by using the bulk modulus of 12 GPa for the solid phase (Prasad et al., 2002; Vanorio et al., 2003). Most of our measured data lie above the HS^-. Brine-saturated kaolinite measurement shows bit lower but parallel values to Yin (1992) data and agree well

Table 3
A comparison between physical properties found for both dry and brine-saturated (BS) smectite and kaolinite aggregates as function of effective stresses and porosity

At same vertical effective stress (σ_v')

σ_v' (MPa)	Porosity (%)				V_p (m/s)				V_s (m/s)			
	Smectite		Kaolinite		Smectite		Kaolinite		Smectite		Kaolinite	
	Dry	BS	Dry	BS	Dry	BS	Dry	BS	Dry	BS	Dry	BS
5	61	49	50	32	940	1617	743	1564	526	366	535	467
30	50	39	34	17	1527	1876	1349	1984	951	514	957	772
50	45	36	28	11	1719	1977	1600	2176	1092	589	1104	900

At same porosity (ϕ)

ϕ (%)	Effective stress (MPa)				V_p (m/s)				V_s (m/s)			
	Smectite		Kaolinite		Smectite		Kaolinite		Smectite		Kaolinite	
	Dry	BS	Dry	BS	Dry	BS	Dry	BS	Dry	BS	Dry	BS
55	15	1.5	2	0.052	1281	1540	600	1250*	766	320	440	280*
45	48	10	8	0.5	1700	1670	900	1360*	1080	400	650	340*
30	95*	50	25	3	1880	2000	1280	1500	1270	600	900	450

Data marked by asterisk (*) are derived from extrapolation of polynomial fits.

with kaolinite–water suspension measurements of Vanorio et al. (2003). As the clays become load-bearing as a function of increasing effective stress, the measured values move away from the Hashin–Shtrikman lower bounds.

4.4. Stress–reflectivity relationships: implication for seismic interpretation

Clay minerals are the most abundant constituents of mudstones and shales and their properties are usually oversimplified in geophysics. To utilize seismic waves fully, it is vital to understand what it reveals about rocks. The present study of systematic clay compaction may give information on how to delineate the coupled effect of fluid and clay mineral responses on seismics. For plane wave fronts parallel to a plane interface, the reflection coefficient (R) is given by

$$R = \frac{\rho_2 V_2 - \rho_1 V_1}{\rho_2 V_2 + \rho_1 V_1}, \tag{9}$$

where ρ_1 and ρ_2 are the bulk densities and V_1 and V_2 are either the V_p or V_s above and below the interface. By considering an interface at every 5 MPa stress interval along the stress path from 1 to 50 MPa, we calculated P- and S-wave reflection coefficients (R_p and R_s) for dry and brine-saturated clay mixtures. The calculated R_p and R_s are plotted against the vertical effective stress, and the least squares fit lines are drawn on Fig. 14a and b. The results illustrate that the reflection coefficients of mudstones (both R_p and R_s) are sensitive to clay mineralogy and pore fluids. Reflection coefficients of aggregates of pure smectite, kaolinite and their mixtures vary to some degree in both dry and wet conditions. The R_p and R_s of dry and brine-saturated clay mixtures decrease exponentially with stress. The maximum decreases are observed at low stresses from 1 to 20 MPa and the decrease of R_p and R_s are relatively small for the rest of the stress range up to 50 MPa. The R_p and R_s of dry clay mixtures are nearly identical with increasing stress (Fig. 14a), but the brine-saturated clay mixtures have significant differences between R_p and R_s (Fig. 14b). The R_s is substantially higher than the R_p, being approximately 0.23 at 1 MPa and decreasing exponentially with increasing stress to about 0.02 at 45 MPa. The maximum changes occur for stresses between stresses 1 and 15 MPa at which the R_s is about 0.05. The differences in reflection coefficient for different clay mixtures are larger at low stresses and reduce relatively fast with increasing effective stress. R_p and R_s are higher in kaolinitic-rich samples than the smectitic-rich samples along the whole stress paths for both dry and brine-saturated clay mixtures.

A comparison of R_p and R_s versus vertical effective stress of dry and brine-saturated clay mixtures is shown in Fig. 14c and d. The differences of R_s of dry and brine-saturated clay mixtures are relatively small but the differences of R_p are quite pronounced. The maximum value of R_p (about 0.35) is found in dry clay mixtures at low stresses, while in brine-saturated condition the maximum value of R_p is about 0.15 at the same effective stress (Fig. 14c). R_s vary from 0.45 to 0.25 (Fig. 14d). The R_s is substantially higher than the R_p, being approximately 0.20 at 1 MPa and decreasing exponentially with increasing stress (Fig. 14d). The maximum change occurs between approximately 1 and 10 MPa at which the reflection coefficient is 0.1. At higher effective stress, the difference in reflection coefficient for all clay mixtures becomes small. The reflection coefficients (both R_p and R_s) of brine-saturated clay mixtures are lower than those found in dry clay mixtures. A similar kind of relationship between reflectivity and stress was also pointed out by Toksoz et al. (1976) and Gregory (1976) for dry and brine-saturated sandstones. The lower reflection coefficients found in smectitic mudstone may possibly be a diagnostic criterion to identify the presence of smectite and also high formation pressure.

The laboratory investigation suggests that the smectite content may significantly reduce the seismic properties (velocity, elastic modulus and density) in poorly lithified, clay-rich sediments. This reduction can be sufficient to cause reflection in shaley sequences and make it possible to detect by seismics if a smectite-rich layer within a shale is thick enough for seismic resolution. With better estimates of mudstones composition and in situ fluid pressure, more realistic seismic properties can be calculated. The sensitivity of the reflection coefficient to clay mineralogy clearly indicates an important future direction in seismics for describing shaley horizons for pore pressure prediction and

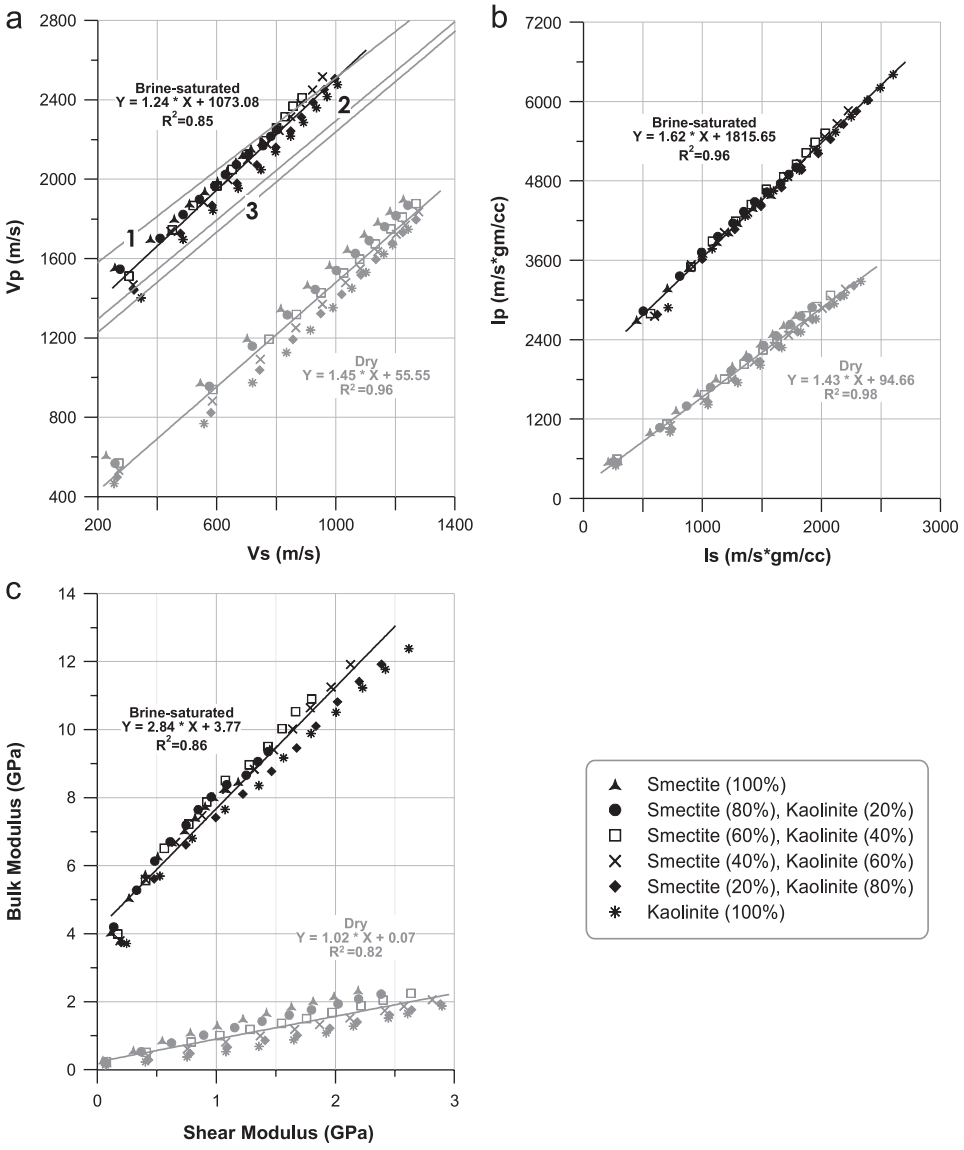

Fig. 12. Cross plots of V_p versus V_s (a), P-impedance versus S-impedance (b) and bulk modulus versus shear modulus (c) for dry (in gray) and brine-saturated (in black) smectite–kaolinite mixtures. The lines show linear fits to the data. The mudrock line (1, Castagna et al., 1985), Castagna et al., 1993; (2) and Han, 1986 (3) empirical relations of V_p and V_s are shown with data measured in this study (a). Equations of best fit lines and correlation coefficient (R^2) are also given with the different plots.

for evaluation of cap rocks. Replacing kaolinite with smectite markedly reduces the elastic moduli of mudstones, and the effect is enhanced at high porosities. At effective stresses greater than about 30 MPa, however, the reflection coefficient becomes essentially independent of the nature of the fluid and clay mineralogy.

5. Conclusions

Experimental clay compaction of smectite and kaolinite mixtures shows large variations in physical properties as functions of composition, effective stress and fluid content. Dry clays are less compressible than wet clays due to higher friction coefficients. The relationships of porosity–effective stress and velocity–effective stress are different for different clay mixtures. Pure smectite is less compressible than pure kaolinite in both dry and brine-saturated states. During the compaction of fine-grained smectitic clays, the effective stress is distributed over a large number of grain contacts compared to other clay minerals resulting in a low overall compressibility, though the strength of the individual smectite grain may be low. The effect of grain size on mechanical compaction is shown in the literature (Skempton, 1953; Mitchell, 1960; Meade, 1964; Chuhan et al., 2003). It is likely that the mechanical compaction found for other clay minerals like chlorite and illite will be intermediate between those found for kaolinite and smectite in this experimental study (Chilingar and Knight, 1960; Meade, 1963; Meade, 1966; Rieke and Chilingarian, 1974). Smectite is found to be the most sensitive clay mineral. Smectitic clays have lower velocity and compressibility as a function of stress/depth and have tendency to

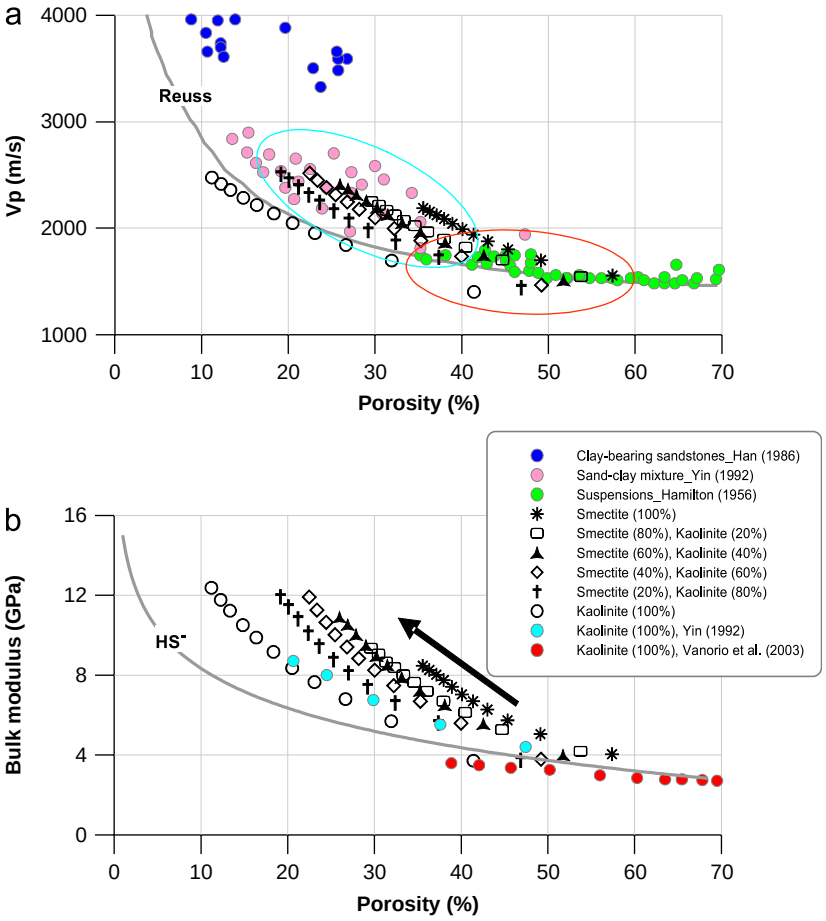

Fig. 13. A comparison of V_p (a) and bulk modulus (b) versus porosity of brine-saturated smectite–kaolinite mixtures (this study) and published data of suspension sediments (Hamilton, 1956), laboratory measured data of sand–clay mixtures (Yin, 1992), clay-bearing sandstones (Han, 1986) and brine-saturated kaolinite (Yin, 1992; Vanorio et al., 2003). Reuss and Hashin–Shtrikman lower bounds are also shown for comparison. The red and cyan ellipses are showing the data range measured at low and medium to high effective stresses (this study). Arrow shows the direction of increasing vertical effective stress.

generate more pore pressure (Fig. 3) during compaction compared to most other clays. Thus, muds with significant smectite content will behave anomalously during mechanical compaction. Our experimental results agree well with data from smectite-rich Tertiary mudstone from the North Sea where well logs documented very low velocity, relatively high porosity and abnormal pore pressures (Bjørlykke, 1998; Thyberg et al., 2000; Storvoll et al., 2005).

Brine-saturated smectitic clays are characterized by low P- and S-wave velocities and high V_p/V_s and Poisson's ratios compared to kaolinitic clays at same effective stress. The elastic moduli of brine-saturated smectitic aggregates are lower compared to kaolinite at the same stress level. This implies that in a sequence of mudstones, smectitic clays will stand out with very different characteristics compared to those of kaolinite and probably also chlorite and illite-rich sequences. On the other hand, at the same porosity, smectitic clays have higher velocities, impedances, elastic moduli and lower V_p/V_s ratios than the kaolinitic clays. This can be explained by the low compressibility, as smectitic clays required significantly higher effective stress to compact to the same porosity level compared to kaolinitic clays (Table 3).

From a comparison between the clay compaction curves reported in this study and other published curves, it can be stated that there is no universal relationship for density, porosity and velocity as a function of burial depth for mudstones and shales. Mudstone compressibility varies within wide limits depending primarily on the types of clay minerals (smectite, kaolinite, chlorite, illite etc.), amount of clays (wt%), other particles (quartz, feldspar, mica, etc.), pore fluids (water, oil or gas) and pore pressure (hydrostatic or overpressure). The mechanical compaction of mudstones is a complex process, and it is not possible to express satisfactorily the porosity/density/velocity versus stress/depth relations by using a single equation. In conclusion, even in pure argillaceous sediments porosity/density/velocity versus stress/depth relations are better expressed by a band than by a line.

It is premature to propose generally valid quantitative relations between stress and volume change in clays and mudstones. There are at the moment too many variables that are not well defined but influence the compaction

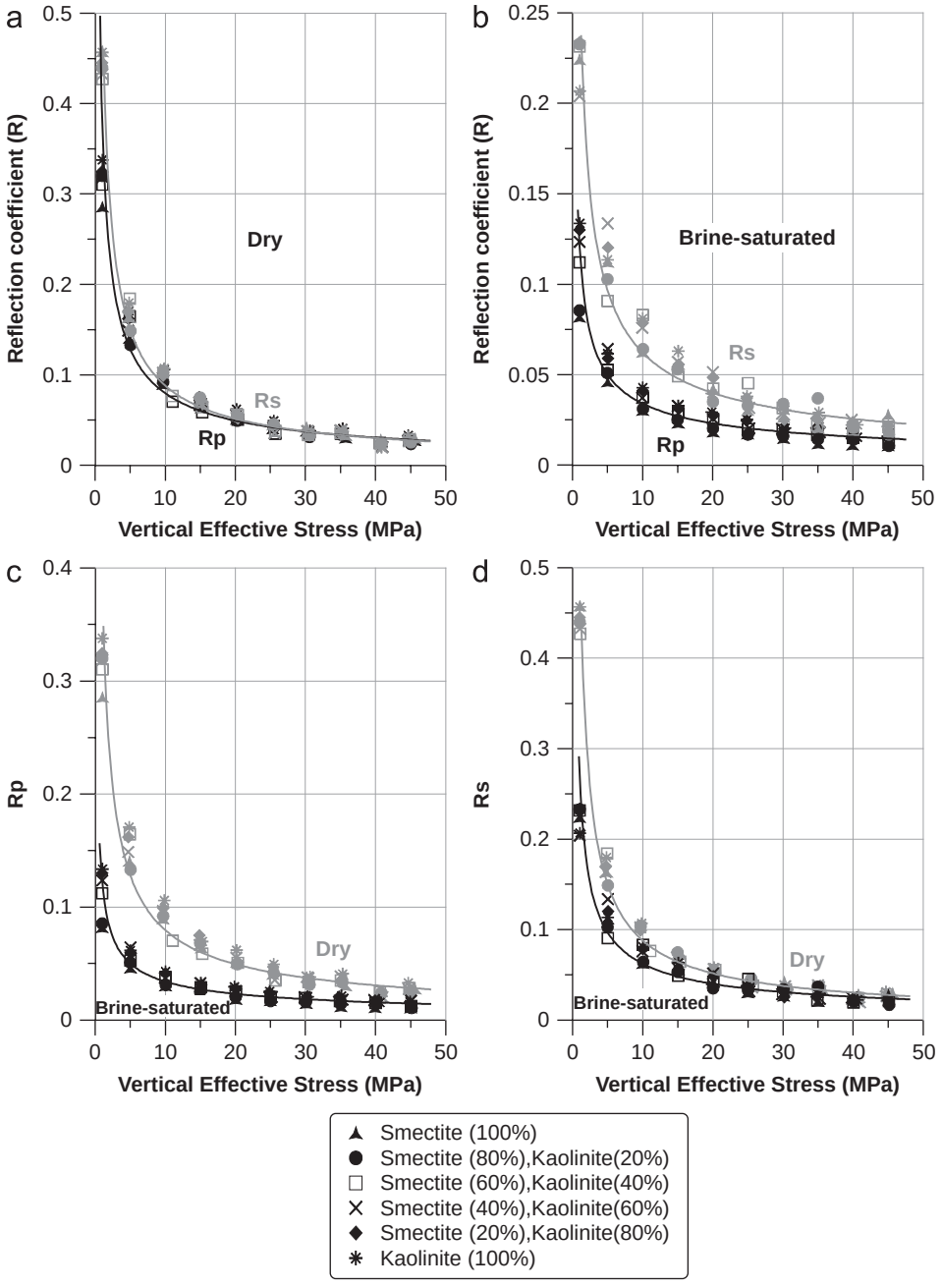

Fig. 14. Cross plots of P-wave reflection coefficient (R_p) and S-wave reflection coefficient (R_s) versus the vertical effective stress for dry (a) and brine-saturated (b) clay mixtures. A comparison of R_p (c) and R_s (d) versus effective stress of dry (in gray) and brine-saturated (in black) clay mixtures are also shown. Black and gray lines show least squares fits to the data.

behavior of argillaceous sediment. The experimental results are valuable but have restricted quantitative application due to the idealized synthetic compositions compared to natural samples. In spite of the limitations, still the present laboratory porosity/density/velocity–stress relations and their comparison with porosity/velocity–depth trends found in well logs will provide important constraints on evaluations of burial depths and/or the amount of uplift and erosion found in sedimentary sequences. The results are of intrinsic value in the interpretation of well log data as well as contributing towards our understanding of the relationships between seismic and petrophysical properties of mudstones, enhancing the accuracy and reliability of the interpretations.

Acknowledgements

Much of this work is supported by the Research Council of Norway (NFR) within the framework of PETROMAKS (Programme for the Optimal Management of Petroleum

Resources) project title "Petrophysical Properties of Mudstones and Sandstones and their Seismic Responses". We acknowledge Statoil for additional financial support. We thank Toralv Berre, Mufak Naoroz, Gudmund Havstad and the technical staff of the Norwegian Geotechnical Institute (NGI) and the Department of Geosciences, University of Oslo, for assistant during the experiments and analyses. Chris B. Peltonen is acknowledged for XRD and XRF analysis of clay samples. Reviewers Andrew Aplin and Quentin Fisher and the Editor in Chief, David Roberts are warmly thanked for helping to improve the clarity of the paper, including the explanation of critical assumptions and the discussion.

References

Alexandrov, K.S., Ryzhova, T.V., 1961. Elastic properties of rock-forming minerals. II. Layered silicates. Bulletin (Izv.) USSR Academy of Science and Geophysical Series 9, 1165–1168.

Anderson, D.L., 1961. Elastic wave propagation in layered anisotropic media. Journal of Geophysical Research 66, 2953–2963.

Aoyagi, K., Kazama, T., Sekiguchi, K., Chilingarian, G.V., 1985. Experimental compaction of Na-montmorillonite clay mixed with crude oil and seawater, Water–rock interaction, vol. 49 (1–3). Elsevier, Amsterdam, Netherlands. pp. 385–392.

Aplin, A.C., Larter, S.R., 2005. Fluid flow, pore pressure, wettability, and leakage in mudstone cap rocks. In: Boult, P., Kaldi, J. (Eds.), Evaluating fault and cap rock seals: AAPG Hedberg Series, vol. 2, pp. 1–12.

Aplin, A.C., Yang, Y., Hansen, S., 1995. Assessment of β the compression coefficient of mudstones and its relationship with detailed lithology. Marine and Petroleum Geology 12 (8), 955–963.

Aplin, A.C., Matenaar, I.F., McCarty, D.K., van Der Pluijm, B., 2006. Influence of mechanical compaction and clay mineral diagenesis on the microfabric and pore-scale properties of deep-water Gulf of Mexico mudstones. Clays and Clay Minerals 54 (4), 500–514.

Athy, L.F., 1930. Density, porosity, and compaction of sedimentary rocks. American Association of Petroleum Geologists Bulletin 14 (1), 1–24.

Ayres, A., Theilen, F., 1999. Relationships between P- and S-waves velocities and geological properties of near-surface sediments of the continental slope of the Barents Sea. Geophysical Prospecting 47 (4), 431–441.

Baldwin, B., 1971. Ways of deciphering compacted sediments. Journal of Sedimentary Petrology 41 (1), 293–301.

Baldwin, B., Butler, C.O., 1985. Compaction curves. American Association of Petroleum Geologists Bulletin 69 (4), 622–626.

Banik, N.C., 1984. Velocity anisotropy of shales and depth estimation in the North Sea basin. Geophysics 49 (9), 1411–1419.

Bayer, U., Wetzel, A., 1989. Compactional behavior of fine-grained sediments; examples from Deep Sea Drilling Project cores. Geologische Rundschau 78 (3), 807–819.

Benson, A.K., Wu, J., 1999. A modeling solution for predicting (a) dry rock bulk modulus, rigidity modulus and (b) seismic velocities and reflection coefficients in porous, fluid-filled rocks with applications to laboratory rock samples and well logs. Journal of Applied Geophysics 41 (1), 49–73.

Berge, P.A., Berryman, J.G., 1995. Realizability of negative pore compressibility in poroelastic composites. Journal of Applied Mechanics 62, 1053–1062.

Biot, M.A., 1956. Theory of propagation of elastic waves in fluid saturated porous solid. Journal of Acoustic Society of America 28, 168–178.

Birch, A.F., 1960. The velocity of compressional waves in rocks to 10 kilobars; Part 1. Journal of Geophysical Research 65 (4), 1083–1102.

Bjørkum, P.A., Oelkers, E.H., Nadeau, P.H., Walderhaug, O., Murphy, W.M., 1998. Porosity prediction in quartzose sandstones as a function of time, temperature, depth, stylolite frequency, and hydrocarbon saturation. American Association of Petroleum Geologists Bulletin 82 (4), 637–648.

Bjørlykke, K., 1997. Predictions of burial diagenetic reactions in sandstones and shales; importance for fluid flow and basin modeling. In: American Association of Petroleum Geologists 1997 Annual Convention, vol. 6. American Association of Petroleum Geologists and Society of Economic Paleontologists and Mineralogists, Tulsa, OK, United States, pp. 11–12.

Bjørlykke, K., 1998. Clay mineral diagenesis in sedimentary basins; a key to the prediction of rock properties; examples from the North Sea Basin. Clay Minerals in the Modern Society, vol. 33(1). Mineralogical Society, London, UK, pp. 15–34.

Bjørlykke, K., 1999. Principal aspects of compaction and fluid flow in mudstones, Muds and mudstone; physical and fluid-flow properties. Geological Society of London, London, United Kingdom 158, pp. 73–78.

Bjørlykke, K., Aagaard, P., 1992. Clay minerals in North Sea sandstones, Origin, diagenesis, and petrophysics of clay minerals in sandstones. Society for Sedimentary Geology (SEPM), Tulsa, OK, United States 47, pp. 65–80.

Bjørlykke, K., Aagaard, P., Dypvik, H., Hastings, D.S., Harper, A.S., 1986. Diagenesis and reservoir properties of Jurassic sandstones from the Haltenbanken area, offshore mid Norway, Habitat of Hydrocarbons on the Norwegian Continental Shelf. In: Proceedings of an International Conference. Graham & Trotman, London, UK.

Blangy, J.P., Strandenes, S., Moos, D., Nur, A., 1993. Ultrasonic velocities in sands; revisited. Geophysics 58 (3), 344–356.

Bolt, G.H., 1956. Physico-chemical analysis of the compressibility of pure clays. Géotechnique 6 (2), 86–93.

Burland, J.B., 1990. On the compressibility and shear strength of natural clays. Géotechnique 40 (3), 329–378.

Callisto, L., Calabresi, G., 1998. Mechanical behaviour of a natural soft clay. Géotechnique 48 (4), 495–513.

Castagna, J.P., Batzle, M.L., Eastwood, R.L., 1985. Relationships between compressional-wave and shear-wave velocities in clastic silicate rocks. Geophysics 50 (4), 571–581.

Castagna, J.P., Batzle, M.L., Kan, T.K., 1993. Rock physics-the link between rock properties and AVO response. In: Castagna, J.P., Backus, M.M. (Eds.), Offset-dependent Reflectivity-Theory and Practice of AVO Analysis. Society of Exploration Geophysicists, Tulsa, OK, United States, pp. 135–171.

Cheng, C.H., Toksoz, M.N., 1976. Pore and crack aspect ratio spectrum determination from seismic velocity data. Eos, Transactions, American Geophysical Union 57 (4), 324.

Chilingar, G.V., Knight, L., 1960. Relationship between pressure and moisture content of kaolinite, illite, and montmorillonite clays. American Association of Petroleum Geologists Bulletin 44 (1), 101–106.

Chilingarian, G.V., Rieke, H.H., 1968. Data on consolidation of fine-grained sediments. Journal of Sedimentary Petrology 38 (3), 811–816.

Chuhan, F.A., Kjeldstad, A., Bjørlykke, K., Hoeg, K., 2002. Porosity loss in sand by grain crushing; experimental evidence and relevance to reservoir quality. Marine and Petroleum Geology 19 (1), 39–53.

Chuhan, F.A., Kjeldstad, A., Bjørlykke, K., Hoeg, K., 2003. Experimental compression of loose sands; relevance to porosity reduction during burial in sedimentary basins. Canadian Geotechnical Journal 40 (5), 995–1011.

Dickinson, G., 1953. Geological aspects of abnormal reservoir pressures in the Gulf Coast Louisiana. American Association of Petroleum Geologists Bulletin 37 (2), 410–432.

Djeran, M.I., Tessier, D., Grunberger, D., Velde, B., Vasseur, G., 1998. Evolution of microstructures and of macroscopic properties of some clays during experimental compaction. Marine and Petroleum Geology 15 (2), 109–128.

Domenico, S.N., 1984. Rock lithology and porosity determination from shear and compressional wave velocity. Geophysics 49 (8), 1188–1195.

Domnesteanu, P., McCann, C., Sothcott, J., 2002. Velocity anisotropy and attenuation of shale in under- and overpressured conditions. Geophysical Prospecting 50 (5), 487–503.

Durmishyan, A.G., 1974. Compaction of argillaceous rocks. International Geology Review 16 (6), 650–653.

Dvorkin, J., Prasad, M., Sakai, A., Lavoie, D., 1999. Elasticity of marine sediments; rock physics modeling. Geophysical Research Letters 26 (12), 1781–1784.

Dzevanshir, R.D., Buryakovskiy, L.A., Chilingarian, G.V., 1986. Simple quantitative evaluation of porosity of argillaceous sediments at various depths of burial. Sedimentary Geology 46 (3–4), 169–175.

Engelhardt, W.V., Gaida, K.H., 1963. Concentration changes of pore solutions during the compaction of clay sediments. Journal of Sedimentary Petrology 33 (4), 919–930.

Faust, L.Y., 1951. Seismic velocity as a function of depth and geologic time. Geophysics 16 (2), 192–206.

Fowler, S.R., White, R.S., Louden, K.E., 1985. Sediment dewatering in the Makran accretionary prism. Earth and Planetary Science Letters 75 (4), 427–438.

Gardner, G.H.F., Gardner, L.W., Gregory, A.R., 1974. Formation velocity and density; the diagnostic basics for stratigraphic traps. Geophysics 39 (6), 770–780.

Gassmann, F., 1951. Elastic waves through a packing of spheres. Geophysics 16 (4), 673–685.

Geertsma, J., 1961. Velocity log interpretation: the effect of rock bulk compressibility. Society of Petroleum Engineers Journal 1, 235–248.

Geertsma, J., Smit, D.C., 1961. Some aspects of elastic wave propagation in fluid-saturated porous solids. Geophysics 26 (2), 169–181.

Goulty, N.R., 1998. Relationships between porosity and effective stress in shales. First Break 16 (12), 413–419.

Grabowska, O.B., 2003. Modelling physical properties of mixtures of clays; example of a two-component mixture of kaolinite and montmorillonite. Applied Clay Science 22 (5), 251–259.

Greenberg, M.L., Castagna, J.P., 1992. Shear-wave velocity estimation in porous rocks; theoretical formulation, preliminary verification and applications. Geophysical Prospecting 40 (2), 195–209.

Gregory, A.R., 1976. Fluid saturation effects on dynamic elastic properties of sedimentary rocks. Geophysics 41 (5), 895–921.

Ham, H.H., 1966. New charts help estimate formation pressures. Oil and Gas Journal 65 (51), 58–63.

Hamilton, E.L., 1956. Low sound velocities in high-porosity sediments. Journal of Acoustic Society of America 28, 16–19.

Hamilton, E.L., 1971. Prediction of in situ acoustic and elastic properties of marine sediments. Geophysics 36 (2), 266–284.

Hamilton, E.L., 1976a. Shear-wave velocity versus depth in marine sediments; a review. Geophysics 41 (5), 985–996.

Hamilton, E.L., 1976b. Variations of density and porosity with depth in deep-sea sediments. Journal of Sedimentary Petrology 46 (2), 280–300.

Hamilton, E.L., Bachman, R.T., 1982. Sound velocity and related properties of marine sediments. Journal of the Acoustical Society of America 72 (6), 1891–1904.

Han, D., 1986. Effects of porosity and clay content on acoustic properties of sandstones and unconsolidated sediments. Ph.D. Thesis, Stanford University, CA, United States.

Han, D., Nur, A., Morgan, D., 1986. Effects of porosity and clay content on wave velocities in sandstones. Geophysics 51 (11), 2093–2107.

Hansen, S., 1996. A compaction trend for Cretaceous and tertiary shales on the Norwegian shelf based on sonic transit times. Petroleum Geoscience 2 (2), 159–166.

Hashin, Z., Shtrikman, S., 1963. A variational approach to the theory of the elastic behaviour of multiphase materials. J. Mech. Phys. Solids 11, 127–140.

Hedberg, H.D., 1936. Gravitational compaction of clays and shales. American Journal of Science 31 (184), 241–287.

Hornby, B.E., 1998. Experimental laboratory determination of the dynamic elastic properties of wet, drained shales. Journal of Geophysical Research, B, Solid Earth and Planets 103 (12), 29,945–29,964.

Hornby, B.E., Schwartz, L.M., Hudson, J.A., 1994. Anisotropic effective-medium modeling of the elastic properties of shales. Geophysics 59 (10), 1570–1582.

Hornby, B.E., Johnson, C.D., Christie, P.A.F., Coyner, K., 2000. Experimental determination of the elastic properties of a compacting fluid-saturated clay, AGU 2000 fall meeting, vol. 81, No. 1. American Geophysical Union, Washington, DC, United States, 1140pp.

Hottmann, C.E., Johnson, R.K., 1965. Estimation of formation pressures from log-derived shale properties. Journal of Petroleum Technology 17, 717–722.

Issler, D.R., 1992. A new approach to shale compaction and stratigraphic restoration, Beaufort-Mackenzie Basin and Mackenzie Corridor, northern Canada. American Association of Petroleum Geologists Bulletin 76 (8), 1170–1189.

Johnston, D.H., 1987. Physical properties of shale at temperature and pressure. Geophysics 52 (10), 1392–1401.

Jones, L.E.A., Wang, H.F., 1981. Ultrasonic velocities in Cretaceous shales from the Williston Basin. Geophysics 46 (3), 288–297.

Jones, O.T., 1944. The compaction of muddy sediments. Quarterly Journal of the Geological Society of London 100 (Part 1 & 2), 137–160.

Kaarsberg, E.A., 1959. Introductory studies of natural and artificial argillaceous aggregates by sound-propagation and X-ray diffraction methods. Journal of Geology 67 (4), 447–472.

Karig, D.E., Hou, G., 1992. High-stress consolidation experiments and their geologic implications. Journal of Geophysical Research, B, Solid Earth and Planets 97 (1), 289–300.

Katahara, K.W., 1996. Clay mineral elastic properties, 66th SEG Annual International Meeting; expanded abstracts, vol. 66. Society of Exploration Geophysicists, Tulsa, OK, United States, pp. 1691–1694.

King, M.S., 1966. Wave velocities in rocks as a function of change in overburden pressure and pore fluid saturants. Geophysics 31 (1), 50–73.

Klimentos, T., 1991. The effects of porosity–permeability–clay content on the velocity of compressional waves. Geophysics 56 (12), 1930–1939.

Kolsky, H., 1953. Stress Waves in Solids. Clarendon Press, Great Britain.

Kowallis, B.J., Jones, L.E.A., Wang, H.F., 1984. Velocity–porosity–clay content systematics of poorly consolidated sandstones. Journal of Geophysical Research. American Geophysical Union, Washington, DC, United States 89 (12), pp. 10,355–10,364.

Krief, M., Garat, J., Stellingwerff, J., Ventre, J., 1990. A petrophysical interpretation using the velocities of P and S waves (full-waveform sonic). The Log Analyst 31 (6), 355–369.

Kuster, G.T., 1977. An interaction model for elastic wave propagation in two-phase media. Geophysical Prospecting 25 (3), 481–495.

Kuster, G.T., Toksoz, M.N., 1974a. Velocity and attenuation of seismic waves in two-phase media; Part I, Theoretical formulations. Geophysics 39 (5), 587–606.

Kuster, G.T., Toksoz, M.N., 1974b. Velocity and attenuation of seismic waves in two-phase media; Part II, Experimental results. Geophysics 39 (5), 607–618.

Lander, R.H., Walderhaug, O., 1999. Predicting porosity through simulating sandstone compaction and quartz cementation. American Association of Petroleum Geologists Bulletin 83 (3), 433–449.

Larsen, G., Chilingar, G.V., 1983. Diagenesis in Sediments and Sedimentary Rocks; 2, Introduction, Developments in Sedimentology 25B. Elsevier Scientific Publishing Co., New York.

Laughton, A.S., 1957. Sound propagation in compacted ocean sediments. Geophysics 22 (2), 233–260.

Lee, M.W., 2003. Velocity ratio and its application to predicting velocities. US Geological Survey Bulletin 2197, 1–15.

Liu, X., Vernik, L., Nur, A., 1994. Effects of saturating fluids on seismic velocities in shale, Society of Exploration Geophysicists, 64th Annual International Meeting; Technical Program, Expanded Abstracts with Authors' Biographies, vol. 64. Society of Exploration Geophysicists, Tulsa, OK, United States, pp. 1121–1124.

Magara, K., 1968. Compaction and migration of fluids in Miocene mudstone, Nagaoka plain, Japan. American Association of Petroleum Geologists Bulletin 52 (12), 2466–2501.

Magara, K., 1980. Comparison of porosity–depth relationships of shale and sandstone. Journal of Petroleum Geology 3 (2), 175–185.

Marion, D., Nur, A., Yin, H., Han, D., 1992. Compressional velocity and porosity in sand-clay mixtures. Geophysics 57 (4), 554–563.

Meade, R.H., 1963. Factors influencing the pore volume of fine-grained sediments under low-to-moderate overburden loads. Sedimentology 2 (3), 235–242.

Meade, R.H., 1964. Removal of water and rearrangement of particles during the compaction of clayey sediments—review US Geological Survey Professional Paper 424-B, pp. B1–B23.

Meade, R.H., 1966. Factors influencing the early stages of the compaction of clays and sands-review. Journal of Sedimentary Petrology 36 (4), 1085–1101.

Mese, A.I., Tutuncu, A.N., 1996. An experimental investigation for relationship between physicochemical and acoustic properties of pure kaolinite and Pierre Shale, 66th SEG Annual International Meeting; expanded abstracts, vol. 66. Society of Exploration Geophysicists, Tulsa, OK, United States, pp. 1695–1698.

Mesri, G., Olson, R.E., 1971. Mechanisms controlling the permeability of clays. Clays and Clay Minerals 19 (3), 151–158.

Mindlin, R.D., 1949. Compliance of elastic bodies in contact. Journal of Applied Mechanics 16, 259–268.

Minshull, T.A., White, R., 1989. Sediment compaction and fluid migration in the Makran accretionary prism. Journal of Geophysical Research, B, Solid Earth and Planets 94 (6), 7387–7402.

Mitchell, J.K., 1960. The application of colloidal theory to the compressibility of clays. In: Parry, R.H.G. (Ed.), Interparticle Forces in Clay–Water–Electrolyte Systems. Commonwealth Science and Industry Research Organization, Melbourne, Australia, pp. 2.92–2.97.

Nafe, J.E., Drake, C.L., 1957. Variation with depth in shallow and deep water marine sediments of porosity, density and the velocities of compressional and shear waves. Geophysics 22 (3), 523–552.

Nobes, D.C., Villinger, H., Davis, E.E., Law, L.K., 1986. Estimation of marine sediment bulk physical properties at depth from seafloor geophysical measurements. Journal of Geophysical Research, B, Solid Earth and Planets 91 (14), 14,033–14,043.

Nygard, R., Gutierrez, M., Gautam, R., Hoeg, K., 2004. Compaction behavior of argillaceous sediments as function of diagenesis. Marine and Petroleum Geology 21 (3), 349–362.

O'Connell, R.J., Budiansky, B., 1974. Seismic velocities in dry and saturated cracked solids. Journal of Geophysical Research 79 (35), 5412–5426.

Olson, R.E., Mitronovas, F., 1962. Shear strength and consolidation characteristics of calcium and magnesium illite, Clays and clay minerals; 9th National Conference of Clays and Clay Minerals. 9.

Pedersen, L., Ryan, S., Sayers, C.M., Sonneland, L., Hafslund, V.H., 1996. Seismic snapshots for reservoir monitoring. Oilfield Review 8 (4), 32–43.

Pickett, G.R., 1963. Acoustic character logs and their applications in formation evaluation. Journal of Petroleum Technology 15 (6), 659–667.

Plona, T.J., Tsang, L., 1978. Characterization of the average microscopic dimension in granular media using ultrasonic pulses; theory and experiments, 48th Society of Exploration Geophysicists Annual International Meeting; expanded abstracts 48, 38–39.

Pouya, A., Irini, D.M., Violaine, L.V., Daniel, G., 1998. Mechanical behavior of fine grained sediments: experimental compaction and three-dimensional constitutive model. Marine and Petroleum Geology 15 (2), 129–143.

Prasad, M., Dvorkin, J., 2001. Velocity to porosity transform in marine sediments. Petrophysics 42 (5), 429–437.

Prasad, M., Kopycinska, M., Rabe, U., Arnold, W., 2002. Measurement of Young's modulus of clay minerals using atomic force acoustic microscopy. Geophysical Research Letters 29 (8), 13.1–13.4.

Proshlyakov, B.K., 1960. Reservoir properties of rocks as a function of their depth and lithology. Geol. Nefti i Gaza 12, 24–29.

Rai, C.S., Hanson, K.E., 1988. Shear-wave velocity anisotropy in sedimentary rocks; a laboratory study. Geophysics 53 (6), 800–806.

Raymer, L.L., Hunt, E.R., Gardner, J.S., 1980. An improved sonic transit time-to-porosity transform, Transactions of the SPWLA 21st Annual Logging Symposium, vol. 21. Society of Professional Well Log Analysts, Houston, TX, United States, pp. P1–P13.

Reuss, A., 1929. Berechnung der Fliessgrenzen von Mischkristallen auf Grund der Plastizitätsbedingung für Einkristalle. Zeitschrift für Angewandte Mathematik und Mechanik 9, 49–58.

Rieke, H.H., Chilingarian, G.V., 1974. Compaction of Argillaceous Sediments, Developments in Sedimentology, Vol. 16. Elsevier, Amsterdam, 424pp.

Rubey, W.W., 1927. The effect of gravitational compaction on the structure of sedimentary rocks; a discussion. American Association of Petroleum Geologists Bulletin 11 (6), 621–632.

Rubey, W.W., Hubbert, M.K., 1959. Role of fluid pressure in mechanics of overthrust faulting. II. Overthrust belt in geosynclinal area of western Wyoming in light of fluid-pressure hypothesis. Geological Society of America Bulletin 70 (2), 167–205.

Sayers, C.M., 1994. The elastic anisotropy of shales. Journal of Geophysical Research, B, Solid Earth and Planets 99 (1), 767–774.

Schreiber, E., 1973. Elastic Constants and Their Measurement. McGraw-Hill Book Co., New York.

Sclater, J.G., Christie, P.A.F., 1980. Continental stretching; an explanation of the post-Mid-Cretaceous subsidence of the central North Sea basin. Journal of Geophysical Research 85 (B7), 3711–3739.

Shumway, G.A., 1958. Sound speed and absorption studies of marine sediments by a resonance method. Ph.D. Thesis, University of California Los Angeles, Los Angeles, CA, United States.

Skempton, A.W., 1944. Notes on the compressibility of clays. Quarterly Journal of the Geological Society of London 100 (Part 1 & 2), 119–135.

Skempton, A.W., 1953. Soil mechanics in relation to geology. Proceedings of the Yorkshire Geological Society 29, 33–62.

Skempton, A.W., 1970. The consolidation of clays by gravitational compaction. Quarterly Journal of the Geological Society of London 125 (Part 3), 373–411.

Storvoll, V., Bjørlykke, K., Mondol, N.H., 2005. Velocity–depth trends in Mesozoic and Cenozoic sediments from the Norwegian shelf. American Association of Petroleum Geologists Bulletin 89 (3), 359–381.

Terzaghi, K., 1925. Principles of soil mechanics: I—phenomena of cohesion of clays. IV—settlement and consolidation of clay. Engineering News-Record 95 (19), 742–746, 874–878.

Thyberg, B.I., Jordt, H., Bjørlykke, K., Faleide, J.I., 2000. Relationships between sequence stratigraphy, mineralogy and geochemistry in Cenozoic sediments of the northern North Sea. In: Nøttvedt, A., Larsen, B.T. (Eds.), Dynamics of the Norwegian Margin. The Geological Society of London, London, United Kingdom, pp. 245–272.

Toksoz, M.N., Cheng, C.H., Timur, A., 1976. Velocities of seismic waves in porous rocks. Geophysics 41 (4), 621–645.

Tosaya, C., Nur, A., 1982. Effects of diagenesis and clays on compressional velocities in rocks. Geophysical Research Letters 9 (1), 5–8.

Tosaya, C.A., 1982. Acoustical properties of clay-bearing rocks. Ph.D. Thesis, Stanford University, Stanford, CA, United States.

Vanorio, T., Prasad, M., Nur, A., 2003. Elastic properties of dry clay mineral aggregates, suspensions and sandstones. Geophysical Journal International 155 (1), 319–326.

Vasseur, G., Djeran, M.I., Grunberger, D., Rousset, G., Tessier, D., Velde, B., 1995. Evolution of structural and physical parameters of clays during experimental compaction. Marine and Petroleum Geology 12 (8), 941–954.

Vassoevich, N.B., 1960. Experiment in constructing typical gravitational compaction curve of clayey sediments. Nov. Neft. Tekh., Geol. Ser. (News Pet. Tech., Geol.) 4, 11–15.

Velde, B., 1996. Compaction trends of clay-rich deep sea sediments. Marine Geology 133 (3–4), 193–201.

Vernik, L., Liu, X., 1997. Velocity anisotropy in shales; a petrophysical study. Geophysics 62 (2), 521–532.

Vernik, L., Nur, A., 1992. Ultrasonic velocity and anisotropy of hydrocarbon source rocks. Geophysics 57 (5), 727–735.

Wang, Z., 2000. Velocity relations in granular rocks. In: Wang, Z., Nur, A. (Eds.), Seismic and acoustic velocities in reservoir rocks, vol. 3. Society of Exploration Geophysics, pp. 377–383.

Wang, Z.Z., Wang, H., Cates, M.E., 2001. Effective elastic properties of solid clays. Geophysics 66 (2), 428–440.

Weller, J.M., 1959. Compaction of sediments. American Association of Petroleum Geologists Bulletin 43 (2), 273–310.

Wijeyesekera, D.C., DeFreitas, M.H., 1976. High-pressure consolidation of kaolinitic clay. American Association of Petroleum Geologists Bulletin 60 (2), 293–298.

Wood, A.W., 1941. A Textbook of Sound. Macmillan Publishing Co, UK.

Wyllie, M.R.J., Gregory, A.R., Gardner, L.W., 1956. Elastic wave velocities in heterogeneous and porous media. Geophysics 21 (1), 41–70.

Xu, S., White, R.E., 1996. A physical model for shear-wave velocity prediction. Geophysical Prospecting 44 (4), 687–717.

Yang, Y., Aplin, A.C., 1998. Influence of lithology and compaction on the pore size distribution and modelled permeability of some mudstones from the Norwegian margin. Marine and Petroleum Geology 15 (2), 163–175.

Yang, Y., Aplin, A.C., 2004. Definition and practical application of mudstone porosity; effective stress relationships. Petroleum Geoscience 10 (2), 153–162.

Yin, H., 1992. Acoustic velocity and attenuation of rocks: Isotropy, intrinsic anisotropy and stress induced anisotropy. Ph. D. Thesis, Stanford University, CA, United States.